

Is Single-View Mesh Reconstruction Ready for Robotics?

Frederik Nolte¹, Bernhard Schölkopf² *Senior Member, IEEE* and Ingmar Posner¹ *Member, IEEE*

Abstract—This paper evaluates single-view mesh reconstruction models for creating digital twin environments in robot manipulation. Recent advances in computer vision for 3D reconstruction from single viewpoints present a potential breakthrough for efficiently creating virtual replicas of physical environments for robotics contexts. However, their suitability for physics simulations and robotics applications remains unexplored. We establish benchmarking criteria for 3D reconstruction in robotics contexts, including handling typical inputs, producing collision-free and stable reconstructions, managing occlusions, and meeting computational constraints. Our empirical evaluation using realistic robotics datasets shows that despite success on computer vision benchmarks, existing approaches fail to meet robotics-specific requirements. We quantitatively examine limitations of single-view reconstruction for practical robotics implementation, in contrast to prior work that focuses on multi-view approaches. Our findings highlight critical gaps between computer vision advances and robotics needs, guiding future research at this intersection.

Index Terms—Computer Vision for Other Robotic Applications; Deep Learning in Robotics and Automation; Object Detection, Segmentation and Categorization; 3D Reconstruction for Real-to-Sim Transfer.

I. INTRODUCTION

RECENT advances in computer vision have produced remarkable improvements in open-vocabulary 3D mesh reconstruction from single image inputs [1]–[3]. These breakthroughs raise a compelling question: can such single-view reconstruction models be leveraged out-of-the-box to create accurate digital twin environments for robotic manipulation without relying on significant post-processing? Although a growing number of recent works employ such 3D reconstruction models, each has limitations in terms of reconstruction accuracy, support for physical simulation, or experimental evaluation [4]–[7]. The ability to efficiently lift real-world observations into accurate simulations could revolutionise how robots interact with and learn from their environments. Single-view approaches are particularly valuable in robotics contexts where collecting multiple viewpoints requires costly physical movement, delays decision-making, or may be entirely infeasible due to environmental constraints or occlusions.

Creating digital twins in simulation – virtual replicas of physical environments – has traditionally been a labour-intensive process requiring specialist training and manually designed assets. This has posed significant hurdles to using simulators in an online fashion such as model-predictive control [8], [9], planning [10], [11], online safety evaluation [12], [13], and real-time learning [14], [15] for robot manipulation, as obtaining accurate state estimations for constructing digital

twin environments in simulation remains non-trivial. A general, automated, and single-view real-to-sim pipeline would map the observed scene into a simulation instance by reconstructing scene objects as individual meshes. If successful, the prospects of scene-agnostic, consistent, and robust dynamics prediction from online observation through simulation are enticing, as these are data-intensive aspects of learned world models [16], [17]. In this work, we formulate desiderata to empirically evaluate whether state-of-the-art single-view reconstruction models are suitable for real-to-sim applications in robotics.

Real-to-sim has received significant attention with several works aiming to leverage recent reconstruction methods in robotics. However, most require dense view-points or scene scans [18]–[28] while the practical limitations of assuming complete scene coverage have not yet been critically examined. Other works rely on only single input views [4]–[7] but only produce domain-randomised environments instead of exact digital twins, do not perform physics simulation, or, while mentioning potential robotics applications, do not describe any robot experiments at all. We describe these works and their limitations in greater detail in Section III-G.

This backdrop of real-to-sim literature motivates the question whether recent advancements in single-view mesh reconstruction models can be effectively applied to create accurate digital twin environments for online, real-time, and high-throughput robotic manipulation. To this end, we formulate desiderata that are particular to robotics and simulation for manipulation and concern the type of input data, computational resources, and overall coherence of the reconstructed scene. We empirically evaluate state-of-the-art 3D reconstruction models against these desiderata by running a series of experiments using data that is typically encountered in robotics deployment scenarios.

Our aim is to guide and inform robotics practitioners and computer vision researchers about existing capability gaps, helping them select tools suited to their tasks while being aware of current limitations. Consequently, inspired by robotics, we are focusing our evaluation on reconstruction models that:

1 Work with single-view image inputs. It is generally impractical to assume that an object can always be observed from multiple meaningful viewpoints a-priori. In some cases, such as entering a new room or opening a drawer, estimating suitable viewpoints and physically reaching them is not trivial due to space constraints and collision avoidance during planning [29], [30]. In other cases, such as books in a shelf, gaining additional viewpoints is impossible without interacting with and rearranging objects in the scene [31]–[33].

2 Produce complete meshes for individual objects. Most robotics simulation engines operate on mesh representations [34]–[36]. While other types of 3D representation, such as point clouds or voxels, are supported in some cases, meshes remain the de-facto standard for rigid body simulation.

¹ Oxford Robotics Institute, University of Oxford. Correspondence to FN. {frederik, ingmar}@robots.ox.ac.uk

² Max Planck Institute for Intelligent Systems & ELLIS Institute Tübingen. bs@tue.mpg.de

3 Are trained to perform open-vocabulary reconstruction.

Historically, 3D datasets have been scarce and small [37]–[39]. As a result, most 3D reconstruction approaches focused on category-specific reconstruction, such as chairs or cars, to limit the task’s scope. This has changed in recent years, with ever-larger 3D datasets [40] and 2D data being used for 3D reconstruction [41], [42]. We are particularly interested in such recent open-vocabulary reconstruction models that promise to produce accurate 3D models of highly heterogeneous object classes, as they allow state estimation in diverse robotics scenarios like households without needing to know a priori what objects are present.

Our systematic evaluation of works fitting these criteria complements existing surveys that attempt to exhaustively *categorise* 3D reconstruction models either generally [43]–[46], or with a focus on specific 3D representations such as NeRFs [47], Gaussian Splatting [48], [49], or Meshes [50], [51]. We are not looking to provide an exhaustive overview of the 3D reconstruction model zoo but instead fundamentally address the question whether single-view reconstruction performance of existing models is sufficient to be used in robotics. [49], [52] offer extensive *overviews* of 3D reconstruction in robotics, but mostly focus on scanning approaches that require substantial scene coverage from the input data stream. In contrast, we focus specifically on single-view reconstruction models and run experiments on real-world datasets to evaluate whether the reported performance on computer vision datasets transfers to realistic robotics domains. [53] have a somewhat similar motivation but focus on three *text-to-3D* generative models, evaluate them towards use in mobile robotics, and investigate several optimisations to improve the latency vs reconstruction quality trade-off. We instead evaluate a broad and representative range of *image-to-3D* models for real-to-sim reconstruction.

In Section II, we delineate desiderata for single-view 3D reconstruction models that robotics domains necessitate. While this is not a survey, we nevertheless provide a brief taxonomy of existing 3D reconstruction approaches in Section III. Even though this work does not focus on multi-view approaches, such works are included for completeness and we refer the reader to relevant surveys, where appropriate. In Section IV, we systematically evaluate a selection of single-view 3D reconstruction models towards these desiderata to see to what extent existing models are readily applicable in the robotics domain. Finally, in Section V we summarise and discuss our findings and position them in the broader context of current research directions.

II. DESIDERATA

For existing open-vocabulary 3D reconstruction models to be effectively integrated into digital twin environments that leverage physics simulators, they must fulfil several key requirements. These requirements ensure that the reconstructed models are not only visually accurate but also physically meaningful, allowing for realistic interactions within a simulation. Furthermore, deployment in the real world results in constraints regarding the available input data and available computational resources. In this section, we motivate several requirements that are key for digital twinning on robotic platforms in the wild.

a) *Reconstruction Accuracy*: Robot manipulation is highly sensitive to accuracy in perceptual system components. For successful robot grasping and manipulation, surface estimates should be within 1mm of the true object surface [54], [55]. Some use-cases, such as assembly or part insertion, can even require sub-millimetre tolerances [56]–[58]. For our evaluation setting of household environments, we set the target accuracy to 2mm.

These stringent accuracy requirements, however, may be challenging to meet with current 3D reconstruction models due to a potential domain gap in training data. Real-world robots are often equipped with RGB-D cameras which offer both RGB and depth perception at relatively low cost [59]. Yet, these cameras typically do not match the resolution and colour profile of images commonly found in 3D reconstruction training datasets [39], [40]. The difference is especially noticeable when an object occupies only a small part of the image plane, as is common when observing an entire scene. Consequently, the 3D reconstruction training data distributions [1], [60], [61] differ substantially from the distribution of inputs encountered during deployment in the real world, potentially resulting in less accurate reconstructions and artifacts [18]. While some approaches like [62] co-train on both real-world images and synthetic data to improve reconstruction accuracy, it remains an open question whether this approach can yield satisfactory results for the precision demands of robotics applications.

Desideratum 1: Chamfer distances between reconstructed and ground truth meshes should be within 2mm. This ensures increased accuracy for household robot manipulation tasks, as well as physical simulation.

b) *Object Collision Constraints*: Physics simulators often use broad- and narrow-phase collision handling to detect collisions between objects’ collision volumes. These collisions are then resolved through penalty- or constraint-based methods that modify the current force acting on the object, its velocity, or its position [34]–[36]. Many 3D reconstruction approaches process objects individually which can result in collisions when placing these reconstructions back into the scene [1], [60], [61]. This is a direct result of insufficient supervision signal from the immediate vicinity of the reconstructed objects. Scenes that collide already during static scene reconstruction fall apart when performing physics steps in the simulator due to the forces and constraints that act upon colliding objects. In principle, one could selectively deactivate collisions between objects to prevent this but that could lead to further complications in downstream simulation and cannot resolve situations where collisions are necessary to preserve the integrity of a scene, such as objects resting on supporting surfaces.

Desideratum 2: No object should violate space occupied by other objects or parts of the environment. This is necessary for the reconstructed scene to be physically stable and to allow for accurate simulation of object interactions.

c) *Object Stability*: This desideratum is based on the assumption that observed scenes are static as long as nothing interacts with them. We can consequently assume that all objects are in a stable, resting state and do not move when advancing simulated physics [63]–[66]. Object pose and an object’s surroundings are necessary conditioning factors as otherwise the reconstruction process could ignore object and scene parts that are critical for object stability in the scene. Especially occluded objects parts and parts with little surface area tend to be ignored during reconstruction, and such inaccuracies can lead to physical instability [63].

Desideratum 3: The reconstructed meshes should offer physically stable poses within 5° tilt of their scene pose, meaning that all objects are in a stable resting state and do not move when advancing simulated physics. This is crucial for ensuring accurate simulation of object interactions and maintaining the integrity of the reconstructed scene.

d) *Partial Occlusion Resolution*: Reconstruction models must accurately resolve partial object occlusions that are ubiquitous in real-world environments [33], [67]. Without proper occlusion handling, digital twins would contain incomplete objects, leading to incorrect simulation physics and failed manipulation attempts. Some 3D reconstruction models run a separate occlusion completion model in their pipeline which can lead to computational overhead and accumulation of reconstruction error [5]. Other works assume that objects tend to be symmetrical or follow other manual shape priors [68], [69]. Object stability, as described in the previous desideratum, can give valuable clues about the structure of occluded parts.

Desideratum 4: The reconstructed meshes should resolve partial occlusions with Chamfer distances no more than 10% higher than those of visible regions when compared to ground truth. This ensures that the reconstructed objects are complete and can be accurately simulated, even in challenging partially-occluded scenarios.

e) *Computational Efficiency*: Many 3D reconstruction models that rely on iteratively optimising a shape representation take several minutes or even hours to reconstruct objects or scenes [1], [63], [66], [70]. As this reconstruction pipeline needs to be run every time a new object is observed, it represents a significant computational cost when deploying (mobile) robots in online environments. Other approaches are able to produce shape reconstructions within few seconds by relying on a single forward pass [2], [60], [71]–[73]. Naturally, latency requirements differ considerably with the type of task that is to be completed. For real-time systems operating at multiple-Hertz frequency [74]–[76], however, these models are likely too slow, especially since compute time accumulates if multiple objects are to be reconstructed. We define a target latency of 2s for reconstructing an entire scene consisting of multiple objects, because the evaluation data used in this paper concerns

less time-critical applications, such as household environments. While one could argue that pre-computing reconstructions and retrieving them from a database when needed might address computational concerns, this approach is generally impractical in online environments like households where object positions, orientations, and even the objects themselves change frequently. Another perspective is given by a possible accuracy/efficiency trade-off, as some computationally more expensive models produce lower-error reconstructions. This would indicate that the practitioner has to make a judgement call as to what reconstruction error and computational cost can be afforded.

Additionally, robots generally have limited on-board compute due to power and payload restrictions [77]. At the same time, many 3D reconstruction models utilise computationally expensive operations, such as diffusion [61], [71] or iterative optimisation [1], [41], [70], rendering them unable to be run on-device without significantly increased latency. Running reconstruction models on dedicated servers and streaming the results to the robotic platform is often not feasible due to latency issues, network dependence, and potential security or privacy concerns [78].

Desideratum 5: The reconstruction pipeline should be able to produce a complete scene reconstruction within 2s, even when multiple objects are present. This ensures that the reconstruction process is efficient and can keep up with the online nature of real-world environments.

III. 3D RECONSTRUCTION - A BRIEF TAXONOMY

While our work is not a survey, it requires us to provide an overview of relevant parts of the literature to motivate our approach and model selection, as well as to position our findings in the broader context of the 3D reconstruction literature. In this section, we present a focused taxonomy of 3D reconstruction approaches. Given the rapidly evolving nature of this research area with new methods appearing frequently, we cannot comprehensively cover all existing approaches. Instead, we focus on representative methods that illustrate key capabilities and limitations relevant to robotic manipulation requirements. This framework highlights how current approaches align with or fall short of the practical needs of robotic systems operating in real-world environments. Specifically, we look at different 3D representations that are used for reconstruction (Section III-A), various input data requirements (Section III-B), different prediction paradigms (Section III-C), different representation abstraction levels (Section III-D), the consideration of physical properties and parameters during reconstruction (Section III-E), training data properties (Section III-F), and how recent reconstruction approaches have been leveraged in a real-to-sim fashion in robotics (Section III-G). Table I gives an overview of a selection of existing reconstruction models and their properties.

A. Types of Representations

Understanding 3D representation types is crucial for evaluating reconstruction methods in robotics, as each representation

influences downstream applications differently. Mesh representations are particularly important for physics simulation in robotics, while point clouds are common from RGB-D sensors. Representation choice affects memory requirements, computational efficiency, and rendering quality – all critical factors for on-robot deployment. Importantly, current robotics simulators are optimised for specific representations (primarily meshes), making representation compatibility a practical necessity rather than just a theoretical concern. 3D representation can be broadly split into two categories: explicit and implicit representations. As some 3D reconstruction models use intermediate representations of different modalities, we briefly explain examples of both explicit and implicit representations.

Explicit representations store each data point individually. **Point clouds**, for example, define surfaces with sets of 3D coordinates $\{x|x \in \mathbb{R}^3\}$ in Euclidean space. Due to the proliferation of RGB-D cameras in robotics [59], point clouds are often readily available in robotics domains and even though they frequently produce artifacts such as holes, they provide comparably more accurate information about scene geometry than 2D RGB projections. Several works propose methods for point cloud estimation or completion [79]–[82]. For a detailed overview of 3D reconstruction with point clouds, see [83]. **Meshes** are among the most widely used 3D representations for simulation as they allow efficient rendering and accurate rigid body collision computation. As a result, simulators are primarily built around mesh representations [35], [36], [84]. Meshes consist of sets of vertices $V = \{v|v \in \mathbb{R}^3\}$, and faces $F = \{(v_n)_{n=0}^N|v_n \in V\}$, surfaces that span subsets of vertices and define the object surface. Due to this very specific structure, directly predicting meshes is non-trivial and existing methods mostly resort to predicting deformation fields on mesh initialisations (e.g. [85]–[87]), or predicting other representations that are subsequently converted into meshes through techniques like ray marching or marching cubes (e.g. [1], [2], [60], [72]). Exceptions include [88], who define a sequential order on the mesh vertices and faces to predict mesh structures with a transformer architecture [89]. Mesh reconstruction from visual observations has received significant attention from the computer vision community [1]–[3], [70]–[72], [87], [90]–[92] and is the main focus of our evaluations in this work due to the widespread support for meshes in robotic simulators. **Gaussian Splatting** [93] is a relatively recent addition to explicit representations. Each Gaussian is defined by its centre position $\mu \in \mathbb{R}^3$, a covariance matrix $\Sigma \in \mathbb{R}^{3 \times 3}$ defining the orientation and shape of the Gaussian blob, an opacity value $\sigma \in [0, 1]$, and its colour. Together, this set of Gaussian blobs defines object surfaces or volumes. Similar to other explicit representations, Gaussian Splatting representations are very efficient to render but come with memory overhead as each Gaussian needs to be stored individually. Due to its high visual fidelity, Gaussian Splatting has recently become a focus for 3D reconstruction [66], [94]–[99].

Implicit representations instead define a function $F : \mathbb{R}^3 \rightarrow I$, where 3D coordinates $x \in \mathbb{R}^3$ are mapped to elements in I . I can have various definitions, such as occupancy $\sigma \in$

$[0, 1]$, colour $c \in [0 - 255]^3$, signed distance $s \in \mathbb{R}$, or any combination of these. The number of parameters in F can be set strictly smaller than the number of coordinates that F is queried with, resulting in a (potentially lossy) compression of the geometric and visual information. At the same time, however, rendering is very inefficient as F has to be queried many times to accumulate geometry and visual information along the camera rays. Specific implicit representation models include Neural Radiance Fields [100] and DeepSDF [101], and Occupancy Networks [102].

B. Input Data

3D reconstruction models can operate on a wide variety of input data modalities. We are concerned with 3D reconstruction in a typical robotics context and focus on reconstruction from image or depth data. For an overview of 3D reconstruction from other modalities such as text, see [103]. 3D reconstruction approaches can be categorised based on the density of input viewpoints required: dense-view, sparse-view, and single-view methods, each with distinct characteristics and applications in robotics scenarios.

Dense-view 3D reconstruction, that is reconstructing only what is observed, has a rich history. If camera poses, projection parameters, and depth data are available, it is straightforward to convert depth information to dense point clouds in the world coordinate system. Without camera extrinsics, reconstruction becomes an optimisation problem. One major line of work, Simultaneous Localisation and Mapping (SLAM), concerns reconstruction of a map of the environment and estimation of the camera trajectory in it from real-time sensor data [104]. Another line of work, Structure-from-Motion, does not operate on online sequential data but instead reconstructs 3D structures and estimates camera viewpoints from unordered sets of offline images [105]. 3D Gaussian Splatting [93], a more recent form of dense-view reconstruction, usually relies on unordered sets of dense views with camera extrinsics available.

Sparse-view reconstruction alleviates the need for complete scene coverage in the reconstruction inputs by leveraging explicit priors, exploiting artifacts in scene representations, or relying on learnt parametric models to complete unobserved regions. [106] utilise explicit priors for volumetric completion while [69] makes assumptions on object smoothness and object-background relations. [68] exploits artifacts resulting from implicit neural representations: as neural networks tend towards smooth function approximation, they observe that implicit neural representations naturally perform object closure and completion to some degree. [107] use parametric models to predict depth and surface normal maps for input images and report increased detail in reconstruction when using these cues. Other works learn parametric models that individually embed multiple views in latent space, fuse these embeddings, and decode towards complete 3D reconstructions [108]–[110]. [99] cluster 3D Gaussians into individual object and complete occluded surfaces using a variational autoencoder [111]. [112] learn a feed-forward model to reconstruct radiance fields from two views and [113] learn a density function over NeRFs that allows image-conditioned sampling with arbitrary numbers of views.

Single-view reconstruction is arguably more difficult for producing faithful reconstructions as substantial portions of a scene are unobserved. Due to this ill-position, proposed methods are trained on datasets to capture general geometric properties of the objects in our world. Single-view reconstruction is particularly central to our work, as it represents the most practical and generalisable scenario for robotic deployment. Unlike multi-view methods that require substantial scene coverage or specialised equipment, single-view approaches align with real-world constraints where robots must rapidly assess and interact with novel environments from limited viewpoints. While these methods traditionally face greater challenges in producing accurate reconstructions, their successful development would enable transformative capabilities for autonomous systems operating in unstructured environments. Broadly speaking, methods can be categorised into two distinct flavours. Firstly, and historically more prominently, there are methods that only rely on the single input view during 3D reconstruction by either directly regressing 3D shapes (for example [95], [114]–[116]) or via test-time optimisation (for example [117]–[119]).

The second popular flavour of single-view 3D reconstruction is leveraging multi-view generative models in the reconstruction process. One way of doing so is explicitly generating additional views based on the input image using multi-view diffusion models, predicting 3D Gaussians for each individual view using a U-Net [3] or transformer [96], and finally fusing the predicted Gaussians. [94] instead use generated views as rendering targets in the original Gaussian Splatting formulation [93]. [71] choose to predict triplane features from multiple artificial views and extract meshes while [2] use a dense set of artificially generated views to predict signed distance values. Multi-view consistency is generally an issue in these approaches as any inconsistencies directly translate to artifacts in the reconstruction. [2] address this by using intermediate cost-volumes that capture inconsistencies. [73] instead fine-tune a multi-view generative model to be more consistent across views, and [61] and [120] propose to condition on a joint feature space derived from multiple views. Some approaches utilise additional information such as albedo or surface normal maps to increase reconstruction fidelity [121], [122]. A separate line of work does not use explicit multi-view generation but instead uses multi-view diffusion models to guide optimisation of an underlying 3D representation [1], [70]. This is explained in more detail in the following Section III-C.

C. Optimisation Paradigms

3D reconstruction can leverage several approaches to arrive at their outputs. Given our interest in robotic applications, the choice of optimisation paradigm is particularly relevant as it directly impacts computational requirements, inference speed, and ultimately the feasibility of on-device deployment. Models with heavy computational demands may be impractical for real-time robotic applications with limited on-board computing resources. In this section, we highlight two primary approaches: feed-forward prediction and inference-time optimisation.

Feed-forward prediction is most in line with the standard use-case of deep learning architectures. For example, [87]

propose a series of convolutional layers to gradually deform ellipsoid mesh initialisations, [114] propose an encoder-decoder structure to predict point cloud coordinates. For a detailed overview of such reconstruction methods up to the year 2021, please refer to [123]. More recently, other models use feed-forward prediction to regress 3D Gaussians: [95] use a U-Net [124] to predict one Gaussian blob per input image pixel while allowing arbitrary position offsets for 3D Gaussians. The simplicity of this architecture enables very fast prediction at up to 38 Hz. [97] instead use transformers to predict 3D Gaussians based on DINOv2 [125] image features and [98] rely on a ResNet-type [126] backbone. Implicit representations can also be produced in a feed-forward manner: [115] learn to regress the parameters of NeRFs using an image-conditioned transformer network while [127] train a diffusion model on NeRF MLP weight matrices. [128] propose a model that maps from image input to triplane features which, when interpolated, can be used to query radiance information at spatial locations. [60] and [72] propose several improvements including data curation, masked losses for higher reconstruction fidelity, material and illumination estimation, and efficient mesh extraction.

A major limitation of feed-forward shape prediction is that 3D datasets have historically been orders of magnitude smaller than their 2D counterparts. This has often limited feed-forward reconstructions to few specific object categories [87], [108], [129] as any attempt at open-vocabulary reconstruction would be too far removed from training distributions. In response to this, several works proposed leveraging pre-trained 2D vision models in a GAN-style [130] setup — training a 3D generative model with guidance through 2D renderings [131]–[133]. Simultaneously, significant efforts have been made towards scaling up 3D datasets [40] which has lead to impressive feed-forward reconstruction performances [116], [134]–[137].

Inference-time optimisation of an underlying 3D representation with guidance signals from pre-trained 2D vision models is an alternative to feed-forward prediction. Some works propose using CLIP [138] to produce gradients on 2D renderings of the underlying 3D asset [118], [119], [139], [140]. If the rendering process itself is differentiable, the chain-rule can be used to obtain gradient signals w.r.t. the 3D representation. However, the bag-of-words behaviour of CLIP models [141] usually limits the visual fidelity. More recently, powerful 2D diffusion models have replaced CLIP in guiding shape optimisation. [42] and [41] both propose a process that repeatedly adds noise to 2D renders of an underlying 3D asset, then uses a pre-trained 2D diffusion model to obtain the 2D score (the gradient of the log-density over the noised 2D image space w.r.t. the 2D image), and apply the chain rule from 2D image to 3D asset to update the asset. An issue with these early diffusion approaches is that the diffusion score cannot be sufficiently guided for multi-view usage — a requirement for making meaningful updates to all parts of the 3D asset. In response, [1] train a view-conditioned 2D diffusion model and increase the 3D reconstruction quality significantly. [70] propose several extensions, including using both 2D and 3D diffusion models and a multi-stage setup. Generally, runtime and memory consumption is a major concern with these approaches, with object generations often requiring multiple hours of optimisation.

D. Representation Abstractions

3D reconstruction approaches can be broadly categorised based on their representational abstraction level. **Wholistic approaches**, including many SLAM systems, typically focus on generating unified representations of entire scenes (e.g. [98], [107], [142]–[144]). These methods generally rely on depth information or estimation to reconstruct observed elements, resulting in representations that essentially project 2.5D information into 3D space.

In contrast, **object-centric approaches** focus on reconstructing individual objects as distinct entities [3], [69], [71], [87], [94]. These methods prioritise resolving self- and viewpoint-occlusion through heuristics or parametric models trained to capture typical object features from datasets.

Between these two extremes lies an emerging middle ground: generating digital twins of entire scenes by fully reconstructing constituent objects while maintaining their individuality [6], [145]–[147]. This hybrid approach is particularly valuable for robotics applications as it enables both scene-level understanding and object-level interaction. Additionally, it allows reconstruction algorithms to leverage contextual information about an object’s surroundings, providing valuable cues about potential occlusions and spatial relationships. For example, proximity between objects suggests possible unseen object parts due to occlusion, rather than assuming these parts simply do not exist because they are not visible in the observation.

E. Physics

Physical plausibility of reconstructed objects and scenes is essential if any physics simulation is to be performed. For rigid bodies, physical plausibility entails aspects of the overall scene composition, such as object collision and stability, as well as physical properties of individual objects themselves.

On the scene level, many approaches formulate loss terms that are incorporated into gradient-based optimisation. For instance, SDF-based representations allow querying whether a particular point in space belongs to the volume of more than one object. As the SDF representation itself is typically optimised with gradient descent, adding a penalty term for doubly occupied space into the overall optimisation is straightforward [148], [149]. [69] and [150] also regularise collision between objects and scene boundaries and background walls by relying on SDFs and bounding boxes, respectively. [151] and [152] take a slightly different approach by not discouraging existing collisions between objects, but instead clustering and decomposing a scene representation into individual objects which naturally addresses object overlap. [6] propose a complex setup that first queries a vision-language model to produce a scene graph containing object-object relations, such as one object supporting another or objects generally being in close contact with one another. Based on these pairwise graph relations, the authors select loss terms from a set of handcrafted loss functions that are then used to optimise physical scene coherence via gradient descent. [146] do not formulate explicit loss terms but instead resolve collisions by coupling the denoising process of multiple objects in their proposed 3D diffusion model, leading to fewer violations.

Instead of handcrafted loss-terms, some approaches resort to differentiable physics simulation. This allows penalising anything that would result in undesirable behaviour during physics simulation, including object collision and object stability – even involving multiple objects at once. [66] dissect single objects into several components, such as a frog wearing a scarf, and optimise component shapes to resolve collision and object stability. [63] perform a similar process on the scene level by reconstructing individual objects and adapting their position and shape such that the resulting scene is physically stable.

Some works do not consider entire scenes or compositional objects but instead concentrate on individual objects only. [91] learn a stability predictor that is used for guiding object reconstruction. [64] formulate differentiable loss terms to optimise stability of single objects. [65] use differentiable simulation during text-to-3D generation for generating stable objects, and [153] augment an SDF decoder with a differentiable simulator for object stability.

Beyond stability and collision, researchers have also looked at estimating object articulations [154]–[156] and material properties [64], [72], [157]. While certainly useful for digital twinning of more complex environments, these aspects go beyond the scope of our study of whether reconstructing physically coherent scenes in simulation for robotics is feasible with current open-vocabulary 3D reconstruction methods.

F. Training Data

Modern AI is heavily data-driven, relying on ever-larger datasets [158]–[160]. In contrast to text and image data, 3D data is not as prevalent on the internet which is the reason why 3D datasets have historically been smaller-scale than their text or image counterparts.

Most existing large-scale 3D datasets are primarily object-centric rather than scene-centric. This focus on isolated objects fails to capture important contextual relationships between objects in realistic environments. For robotics applications seeking to create accurate digital twins of entire scenes, having training data that represents realistic object arrangements, support relationships, and partial occlusions is crucial. Scene-level data would allow reconstruction models to learn typical object configurations and physical constraints that govern real-world environments. Without such contextual learning, models struggle to produce physically plausible reconstructions of complex scenes, leading to the stability and collision issues we observe in our evaluations.

Object Datasets: ShapeNet [37] has been very influential ever since its introduction, offering around 51k 3D object models in its curated form. Still, it does not offer enough breadth and detail to allow for training open-vocabulary reconstruction models and as a result, most proposed reconstruction methods focused on few specific categories, such as cars or chairs [87], [108], [129]. More recently, OmniObjects3D [39] and GSO [161] proposed highly-detailed 3D object datasets, albeit at a smaller scale than ShapeNet. In 2023, Objaverse-XL [40] presented an inflection point for 3D datasets, offering over 10 million highly-diverse 3D models. For the first time, 3D

reconstruction models trained on this dataset made the value proposition of being able to reconstruct ‘any’ object [1]. A recurring theme among large-scale 3D datasets is the reliance on synthetic object rendering. With robotics being an area that is heavily concerned with the Sim2Real gap, including subtle differences between renderings and real-world camera footage [162], relying solely on simulated training data might not translate to good downstream performance.

Scene Datasets: Regarding scene-level datasets, the focus is not on object diversity but rather on diversity of scene layout and composition. Similar to object-centric datasets, scene-level datasets can be synthetic and potentially procedurally generated [163]–[166]. Procedural generation allows theoretically infinite scene layouts from a finite set of objects. Other datasets focus on manually obtained 3D scans of real scenes [167]–[169]. Due to the scanning process that is used for obtaining these datasets, one could say they are not truly 3D but only a collection of 2.5D information. As a result, the collected scenes frequently contain holes and do not feature complete object meshes. Instead, they only reconstruct what has been scanned. [170] provide a collection of 3D scenes featuring YCB objects [171], a collection of common household objects that are frequently featured in robot experiments [172]–[174]. Recently, [175] proposed a richly annotated digital twin dataset comprised of two indoor scenes.

G. Applications in Robotics

In this section, we focus our attention on 3D reconstruction for creating digital twin environments to support robot manipulation. Reconstruction has had a major role in robotics research and a great many literature reviews have been published that discuss several areas in greater detail, including SLAM [176], [177], 3D Gaussian Splatting [49], as well as neural fields [178] for robotics tasks such as navigation and manipulation. We organise this section into two main categories. For completeness, we include dense- and multi-view reconstruction methods which have had a long history in robotics, while single-view reconstruction methods are more recent and the primary focus of the rest of this paper.

Dense- and Multi-View: 3D reconstruction from dense viewpoints has been extensively used in robotics, for example, SLAM is frequently used in mobile robotics and navigation [179]–[181]. Closer to our real-to-sim setup, 3D Gaussians have recently been adopted for Real2Sim2Real in robotics [18]–[25]. Typically, 3D Gaussians are learnt alongside coupled mesh representations of objects from dense view points. The 3D Gaussians are used for realistic rendering to close the sim-to-real gap, while the mesh-based representations are used for rigid body simulation. The resulting pipeline can be used for trajectory augmentation and reinforcement learning in simulation. Instead of a dual mesh representation, [182] use a particle-based representation and simulator while also relying on 3D Gaussians for rendering fidelity.

[26] propose a similar pipeline but instead of relying on dual representations tied to 3D Gaussians, they only reconstruct scene meshes by densely scanning the scene and relying on human annotations. Again, the pipeline is used

for reinforcement learning in simulation. Similarly, [27] also forego Gaussian Splatting to instead reconstruct object meshes obtained from dense input viewpoints. [28] technically only require a single camera viewpoint for reconstructing mesh representations from object observations but rely on a robotic arm to present the object from different angles and re-grasp it to reduce occlusions.

While certainly pushing the state-of-the-art of real-to-sim capabilities in robotics, these methods all require substantial scene coverage in their input data. This is a major limitation that as of yet has to be critically examined in the literature. Dense observations are not always available in real-world scenarios, especially when dealing with unstructured environments or when the robot is required to operate quickly. This limitation highlights the need for reconstruction methods that can effectively operate with limited input data, such as single-view reconstruction methods.

Single-View: Recent open-vocabulary single-view reconstruction methods have been proposed for robotics applications, but the focus has been very limited. Existing works face several limitations, such as having to learn dynamics models, not reconstructing exact digital twins, or only considering the reconstructed scene as a static entity without simulation.

[4] propose generating digital twins from single image observations for robotic learning. However, they do not produce exact digital twins but instead insert a language and 2D image generation model into their pipeline. These are then used for generating diverse sets of objects similar to the observed objects, which are assembled into domain-randomised environments for use in downstream tasks. In addition to not producing exact digital twins, their method relies on a commercial reconstruction model, is only evaluated on very simple tabletop scenes without occlusion, and does not explicitly address object collisions resulting from reconstruction. [5] pose the question whether single-view object-centric 3D reconstruction of entire scenes can be used in robotics. They show that using only pre-trained models, one can produce digital twins that afford computing parallel grasp poses that transfer to the real-world scene. However, they do not perform any form of simulation on the reconstructed scene. [6] propose generating digital twins of entire scenes from single-view observation while also addressing physical constraints such as object collision and stability. Their process relies on GPT-4v [183] to produce accurate scene graphs that are used in their gradient-based physics optimisation. While stating that their approach enables Real2Sim transfer for robotics, the authors do not provide any experimental evaluation for this claim. Similarly, [7] mention their generative approach for domain randomisation could be used for creating digital twin environments for robotics but no further details or experimental evaluations are provided.

Different from the above mesh reconstruction approaches, [184] produce 3D Gaussians while only requiring a single input view. However, as existing robotics simulators do not support 3D Gaussians, the authors propose to learn a neural dynamics model instead.

Our work addresses an important gap in the literature by conducting a rigorous empirical evaluation of single-view reconstruction methods specifically in the context of robotics

requirements. We focus on evaluating whether recent advances in computer vision for single-view 3D reconstruction can actually meet the particular needs of robotics simulation, providing concrete evidence of their current limitations and identifying specific areas for improvement.

IV. MODEL EVALUATION AND RESULTS

As the field of 3D reconstruction is growing rapidly, we select the following representative set of object- and scene-level reconstruction methods. For a short description for each selected model, see Appendix A.

a) *Object-Level Reconstruction Models*: SF3D [72], InstantMesh [116], One2345 [2], LGM [3], Michelangelo [195], ZeroShape [134], Real3D [62], and DSO [191].

b) *Scene-Level Reconstruction Models*: MIDI [146], Gen3DSR [145], and PhysGen3D [198].

Since we are interested in estimating the Lagrangian state from visual observation, we do not consider methods that generate 3D structures only from text input (e.g. [42], [65], [92]). Furthermore, given our focus on single-view reconstruction, we do not evaluate models that require multiple viewpoints (e.g. [68], [69], [96], [107], [121], [136], [148]) or even dense observations (including [18]–[28], [63], [143], [182], [203], [204]). Most established simulation engines in robotics require mesh representations of objects. At the same time, converting 3D Gaussians to mesh surfaces is not a trivial operation [205]. To fairly assess reconstruction performance, we opt to only consider methods that either produce meshes themselves or come with pre-defined mesh extraction routines. Further, optimisation-based routines such as score distillation are slow by design. Since we are concerned with computational requirements and responsiveness during reconstruction (Section II-0e), we do not consider such methods in our experiments (including [1], [61], [65], [70], [120], [189], [190], [200], [206], [207]). Finally, while we generally outline potential issues with offloading compute from the robot platform to cloud services in Section II-0e, we are practically limited to evaluating methods that have open-source implementations available.

For an in-depth overview, including the required number of viewpoints, asset and optimisation type, as well as physics considerations of reconstruction methods including those we experimentally evaluate, see Table I.

A. Evaluation Data

To properly evaluate reconstruction methods, we require richly annotated real-world data. However, most scene-level datasets for reconstruction or SLAM only contain 2.5D information [167], [208], [209]. We select two datasets in our experiments: parts of the YCB-Video dataset [170] and the Project Aria Digital Twin dataset [175]. These datasets are particularly representative for robotics applications as they capture different aspects of the challenges faced in real-world manipulation tasks. The YCB-Video dataset features standardised objects with varying geometric complexity that have become benchmarks in the robotic manipulation community, while the Aria dataset contains everyday household items arranged in naturalistic

configurations that robots would encounter in domestic environments. Together, they span a spectrum from controlled, well-defined object arrangements to complex, cluttered real-world scenes. Both datasets provide ground-truth meshes for all objects, their poses in each camera frame, and additional information such as segmentation masks and camera intrinsics of their respective camera types. This rich annotation is crucial for quantitatively evaluating reconstruction accuracy against true object geometry. See Figure 16 for example inputs from both datasets. For both datasets, we manually select objects and frames to ensure coverage of different object types, camera view-points, and object poses.

B. Experimental Methodology

Each reconstruction model is evaluated on the same set of objects and camera frames. As all evaluated methods are single-view reconstruction approaches, we provide them with a single image of the object to be reconstructed. For each method, we follow the provided data preparation routing, including cropping and resizing of the object to a common size in the image frame. For all methods that rely on off-the-shelf segmentation models in their pipeline, we provide ground-truth object masks during the reconstruction process. This is done to ensure a fair and consistent comparison independent from off-the-shelf methods.

To evaluate reconstruction error, we need to align the reconstructed mesh to the ground truth. Past works [2], [191] have used alignment procedures that we extend as follows. First, we estimate the correct scale of the object. To do this, we compute the standard deviations of the mesh vertices along the top three principle components of each mesh. We then evaluate the ratio of the component-aligned standard deviations of the ground truth mesh w.r.t. the reconstruction and estimate the rescaling parameter as the median of these principal component-aligned ratios.

To align translation and rotation, we sample 512 approximately equidistant unit quaternions from the 3-sphere and use these as initialisations for an iterative closest point (ICP) optimisation. The large number of initialisations is chosen to avoid local optimisation optima. We then select the transformation with the lowest root mean squared error among all initialisations.

In our evaluations, we mainly rely on the Chamfer distance (CD) as a measure of reconstruction error. This is in line with recent reconstruction works [1], [71], [128], [191]. We follow the implementation of [102] for computing the Chamfer distances.

C. Results

To evaluate how well current single-view 3D reconstruction methods meet the robotics-specific desiderata outlined in Section II, we systematically assess each requirement using our experimental pipeline. Our evaluation focuses on understanding whether these methods can produce reconstructions that are sufficiently accurate, physically plausible (collision-free and stable), capable of resolving occlusions, and computationally efficient. The following results, organised by each desideratum, reveal significant gaps between current capabilities and the requirements for effective robotic applications.

TABLE 1
RELEVANT SINGLE-VIEW 3D RECONSTRUCTION MODELS AND THEIR PROPERTIES.

Paper	Input Viewpoints	Depth Input	Reconstruction Level	Asset Type	Optimisation Type	Object Decomposition	Physics	Open Source
[150]	Single	Pretrained	Scene	Mesh	Feed-Forward	Yes	Object Collision	No
[97]	Single	No	Object	3D Gaussians	Feed-Forward	No	No	No
[185]	Single	No	Object Scene	Field, Mesh	Feed-Forward	Segments single foreground object	No	No
[144]	Single, Multi	No	Scene	3D Gaussians	Feed-Forward	No	No	No
[186]	Single	Pretrained	Scene	Voxel	Feed-Forward	Yes	Objects cannot collide as scene is represented by voxels	Yes
[6]	Single	Pretrained	Scene	Mesh	Iterative Feed-Forward (Object Reconstruction), GPT-4v (Scene Graph), Gradient-Descent (Physics Optimisation)	Yes	Collision and Stability	No
[187]	Single	Yes	Object	Mesh	Feed-Forward	No	No	No
[188]	Single	Custom	Object	3D Gaussians, Mesh	Feed-Forward	No	No	No
[135]	Single	No	Object	NeRF, Mesh	Feed-Forward	No	No	No
[189]	Single	Pretrained	Object	Implicit Surface, Mesh	Gradient-Descent (Score Distillation)	No	No	Yes
[190]	Single	No	Object	3D Gaussians, Mesh	Gradient-Descent (Score Distillation & Texture Refinement)	No	No	Yes
[191]	Single	No	Object	Mesh	Feed-Forward	No	Fine-tuned to predict stable object	Yes
[98]	Single	Pretrained	Scene	3D Gaussians	Feed-Forward	No	No	Yes
[192]	Single	No	Object	3D Gaussians	Feed-Forward	No	No	Yes
[145]	Single	Pretrained	Scene	Mesh	Gradient-Descent (Score Distillation) by default; can be combined with other models	Yes	No	Yes
[96]	Single	No	Object	3D Gaussians, Mesh	Feed-Forward	No	No	No
[149]	Single	No	Scene	SDF, Mesh	Feed-Forward, Iterative Refinement	Yes	Collision	Yes
[94]	Single	No	Object	3D Gaussians	Feed-Forward (Video Gen), Gradient-Descent (3D Gaussians)	No	No	No
[116]	Text, Single, Multi	No	Object	Triplane, NeRF, Mesh	Feed-Forward	No	No	No
[71]	Single	No	Object	Mesh	Feed-Forward	No	No	Yes
[95]	Single	No	Object	3D Gaussians	Feed-Forward	No	No	No
[3]	Single	No	Object	3D Gaussians, Mesh	Feed-Forward	No	No	Yes
[128]	Single	No	Object	NeRF, Mesh	Feed-Forward	No	No	No
[70]	Single	No	Object	Mesh	Gradient-Descent (Score Distillation)	No	No	Yes
[94]	Single	No	Object	Mesh	Feed-Forward	No	No	No
[95]	Single	No	Object	Mesh	Feed-Forward	No	No	No
[146]	Single	No	Scene	SDF, Mesh	Feed-Forward	Yes	Soft Collision	Yes
[96]	Single	Yes	Object Scene	Point Cloud	Feed-Forward	No	No	Yes
[120]	Single	No	Object	NeRF	Gradient-Descent (Score Distillation)	No	No	Yes
[197]	Single	Pretrained	Scene	Mesh	Feed-Forward	Yes	Collision	No
[2]	Single	No	Object	SDF, Mesh	Feed-Forward	No	No	Yes
[73]	Single	No	Object	SDF, Mesh	Feed-Forward	No	No	No
[66]	Single	No	Object	3D Gaussians	Feed-Forward (Multi-View Gen), Gradient-Descent (SDF, Score Distillation, Diff'ble Physics Simulation)	Single object into 2 components	Full Simulation	Yes
[198]	Single	Pretrained	Scene	Mesh	Feed-Forward (Reconstruction), GPT-4o, Gradient-Descent (Diff'ble Renderer)	Yes	Reconstructions can be used in particle simulator but stability and collision play no role during reconstruction process.	Yes
[153]	Single	No	Object	SDF	Feed-Forward (SDF), Gradient-Descent (Diff'ble Physics Sim)	No	Stability	No
[64]	Single	No	Object	Mesh	Gradient-Descent	No	Stability, Mechanical Material Properties	Yes
[62]	Single	No	Object	Mesh	Feed-Forward	No	No	Yes
[147]	Single	Pretrained	Scene	Mesh	Gradient-Descent (Score Distillation & Diff'ble Rendering for Poses)	Yes	No	Not functional
[72]	Single	No	Object	Mesh	Feed-Forward	No	No	Yes
[127]	Single	No	Object	NeRF, Mesh	Feed-Forward	Yes	No	Yes
[199]	Single	No	Scene	Mesh	Feed-Forward	Yes	No	Yes
[93]	Single	No	Object	3D Gaussians	Feed-Forward	No	No	Yes
[200]	Single	No	Object	Mesh	Feed-Forward (Multi-View Gen), Gradient-Descent (Score Distillation)	No	No	Yes
[61]	Single	No	Object	Mesh	Feed-Forward	No	No	Yes
[115]	Single	No	Object	NeRF	Gradient-Descent (Score Distillation)	No	No	Yes
[137]	Single	No	Object	3D Gaussians	Feed-Forward	No	No	Yes
[122]	Single	Custom	Object	Mesh	Feed-Forward	No	No	Yes
[201]	Single	No	Object	Point Cloud	Feed-Forward	No	No	Yes
[202]	Single	No	Object	Mesh	Feed-Forward (Multi-View Gen), Gradient-Descent (SDF)	No	No	Yes
[1]	Single	No	Object	Mesh	Gradient-Descent (Score Distillation)	No	No	Yes
[134]	Single	Custom	Object	Mesh	Feed-Forward	No	No	Yes

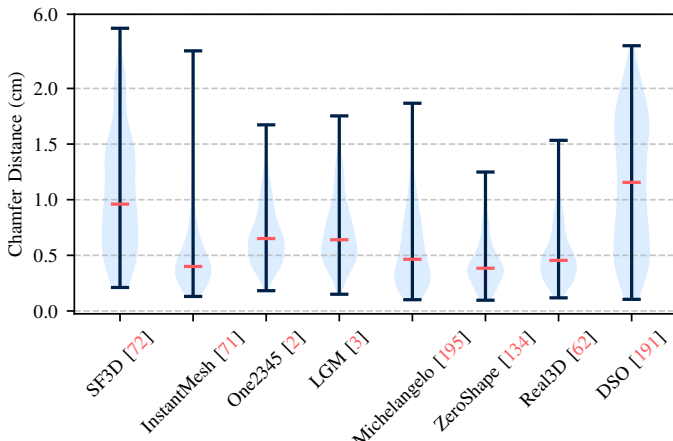


Fig. 1. Reconstruction error on the YCB-Video [170] dataset as measured by the Chamfer distance (CD). CD is averaged across 10,000 sampled surface points from both target and reconstruction. Indicators for min, max, and median are shown. For most methods, reconstructed surfaces are about 5mm distant from the closest target mesh surface.

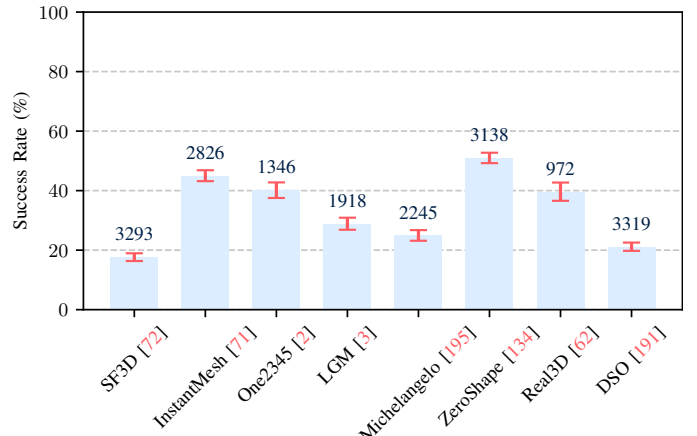


Fig. 2. Success rates of transferring grasp poses computed on the reconstruction to the target mesh. Indicated are 95%-confidence Wilson intervals and the number of successfully sampled grasps. Evaluated on the YCB-Video [170] dataset. The object reconstructions of which the Chamfer distances are reported in Figure 1 are too inaccurate to successfully transfer grasp poses from reconstruction to the target meshes. As a result, grasps that are computed and evaluated in simulation do not normally transfer to the real world.

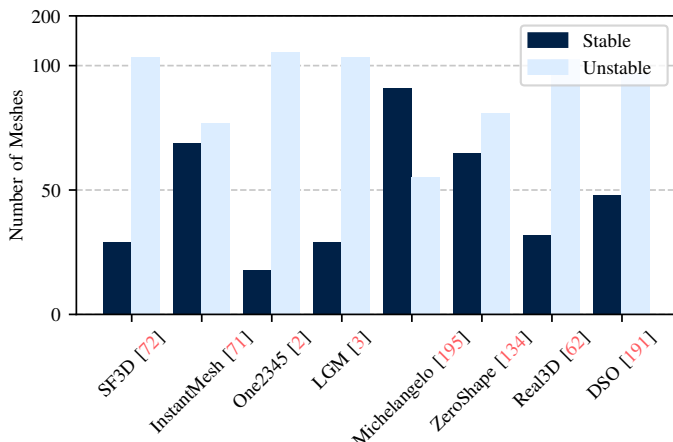


Fig. 3. Total number of objects with physically stable poses within 5° from the ground truth scene pose versus total number of objects without such stable poses. Evaluated on YCB-Video. For results on the Aria Digital Twin [175] dataset, see Figure 14. Object mesh reconstructions from all methods exhibit significant physical instability, with many objects unable to maintain proper positioning in physics simulations. Consequently, these scene reconstructions would collapse or disintegrate when subjected to physical simulation environments.

a) Reconstruction Accuracy: To evaluate how accurately popular reconstruction models produce 3D reconstructions when queried with imagery that reflects realistic robotic observations, we run all models on segmented objects that are entirely visible except for self-occlusion. We select 177 such objects from YCB-Video and 136 objects from the Aria dataset. As there are no guarantees that reconstructed meshes are valid volumes, we evaluate reconstruction accuracy by uniformly sampling 10,000 points from the surfaces of ground truth mesh and reconstruction, and computing the Chamfer distance (ℓ^2 -norm) between both point clouds.

Figures 1 and 13 depict the resulting Chamfer distances for the single-object models on the two datasets. On YCB-Video [170], with the exception of SF3D [72] and DSO [191], reconstructed surfaces tend to be about 5mm distant from the closest surface in the ground truth meshes. Reconstruction accuracy on the Meta Aria Digital Twin [175] dataset is signifi-

cantly worse, with about double the median reconstruction error. Figure 16 depicts a collection of example scenes alongside mesh reconstructions to give the reader an impression of the visual manifestation of such error ranges. Models appear to especially struggle with objects in non-canonical poses, such as view-points towards the top or bottom of the object. Such reconstruction error would result in very different behaviour than the ground truth object, if put into a physics simulator. Further, we evaluate the transfer success rates of grasp poses computed on reconstructions to the ground truth meshes on YCB-Video [170]. The results in Figure 2 indicate that the reconstructed meshes are insufficiently accurate for computing grasp poses on the reconstructed meshes and applying them in the real world scene — only about a third of all grasp poses can successfully be applied to the target meshes. For grasp sampling, we use the antipodal grasp sampling procedure presented in [210] with a Franka Emika Panda parallel gripper model. Grasp poses computed on the reconstructions are considered to transfer successfully if they are not in collision with the ground truth mesh, and the rotations between gripper surface normals and mesh surface normals at the grasp points are not in excess of 22.5° , as specified in the implementation of [210].

To evaluate the reconstruction quality of models that process entire scenes, we select 28 scenes from the YCB-Video [170] dataset, sample 10,000 points each from the reconstructed and ground truth surfaces of the *entire* scene, align the reconstructed scene *as a whole* with the target scene using the ICP process described in Section IV-B, and compute the Chamfer distances between reconstruction and target, as we have done in the single-object case. Figure 5 shows that models that reconstruct entire scenes perform worse on average than single-object reconstruction models. With the median error being between 1cm and 1.5cm, the reconstructed scene and its objects would behave very differently when used in a physics simulation. Such error ranges are too large for robust robotic manipulation and miss our formulated reconstruction target of 2mm by a large margin. Figure 10 separately evaluates the pose estimation

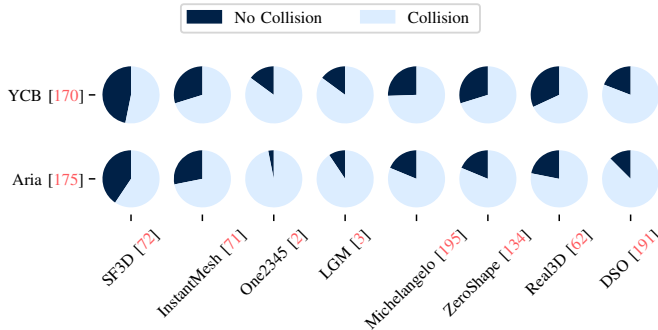


Fig. 4. Frequency of reconstructed scenes where reconstructed meshes are in collision with one another. Objects being more frequently in collision than not results in unwanted behaviour in physics simulation, such as instantaneous acceleration and collapse of the scene composition. As a result, these reconstructions are not suitable for use in robotics simulation. As the reconstruction models in this figure only operate on individual objects, this may well be outside the scope of these models. As we show in Figure 12, scene-level reconstruction models tend to produce fewer collisions.

of scene reconstruction models by looking at the relative Chamfer distance between two objects in the reconstruction and computing the difference to the relative distance between the same objects in the ground truth scene. The results show that the relative object poses are not preserved in the reconstruction, which is a requirement for both accurate physics simulation and being able to transfer manipulation trajectories from simulation to the real world. Figure 17 depicts several reconstruction examples of the scene-level models. It is clear that both reconstruction accuracy of individual objects as well as pose estimation is suboptimal.

b) Object Collision Constraints: To evaluate how often inaccurate reconstructions result in mesh collisions, we select object pairs that are spatially close, reconstruct them individually, place them at their respective scene poses obtained through the ICP procedure described in Section IV-B, and use FCL [211] to compute mesh collisions between them. The evaluation dataset consists of 96 samples for YCB-Video [170] and 64 samples for the Meta Aria Digital Twin [175] dataset.

Figure 4 shows that all single-object reconstruction models produce meshes that are in collision in a majority of the evaluation scenes. If used in a physics simulation, such collisions at initialisation would result in unwanted behaviour, such as instantaneous acceleration and collapse of the scene composition. Figure 12 shows that even though scene reconstruction models operate on entire scenes and thus in principle should be in a good position to avoid mesh collisions in their reconstructions through conditioning one object’s reconstructed mesh on other objects’ scene occupancy, as well as having control over the positioning of individual objects, their ability to avoid mesh collisions is only on par with the better single-object models. Only PhysGen3D shows vastly reduced mesh collisions. However, this may be an artifact of the model significantly overestimating relative object distances (Figure 10) which would automatically result in reduced object collisions.

c) Object Stability: To evaluate whether reconstructed objects would be stable when put back into the scene, we first compute their stable orientations, that are all orientations where the centre of mass is within the 2D convex hull of vertices that have minimal elevation. We then filter for those

stable orientations where the z-axis is at most 5° tilted from the z-axis of the object in the scene, i.e. where the stable pose is similarly upright as the object in the scene. For each of the resulting candidate poses, we generate 8 equally spaced perturbations that rotate the object 5° away from its stable pose. If in a subsequent physics simulation using PyBullet [35] at least one of these perturbed poses leads to the object reverting back to the unperturbed pose, the unperturbed pose is considered stable. As a result, we obtain all poses that are physically robust to slight perturbation while also being close to the ground truth pose of the object in the scene. In our evaluation, we only consider objects that are resting on planes, not ones that are leaning against other objects. We use 146 samples from YCB-Video [170] and 133 samples from the Meta Aria Digital Twin [175] dataset.

Figure 3 shows that the vast majority of YCB-Video reconstructions does not have stable poses near the observed scene pose. Michelangelo [195] stands out among all other evaluated models with two thirds of the reconstructed meshes having valid stable poses. On the Meta Aria Digital Twin [175] dataset, however, Michelangelo does not show the same advantage. Instead, all evaluated models produce even fewer stable mesh reconstructions than on YCB-Video. As a result, the reconstructed meshes would be largely unusable for physics simulation without significant, non-trivial postprocessing, as without it the object meshes would topple over as soon as physics steps are advanced.

Figure 7 shows that the scene reconstruction models do not fare any better. Instead, PhysGen3D [198] shows the least number of stable meshes among all evaluated models. To evaluate whether the reconstructed meshes themselves or the pose estimation of the scene reconstruction models are to blame, we align each reconstructed object mesh with the ground truth mesh separately and compute the number of stable poses again. The results are shown in Figure 8. The number of stable poses increases significantly, corroborating that the scene reconstruction models struggle to estimate the correct object poses. Still, the number of stable poses remains too low for practical use in robotics applications.

d) Partial Occlusion Resolution: To evaluate how well reconstruction models are able to resolve occlusions, we select a subset of 80 partially occluded objects from YCB-Video [170] dataset and a subset of 76 partially occluded objects from the Meta Aria Digital Twin [175] dataset. During the evaluation, we noticed that many methods struggle with reconstructing occluded object parts and often ignore such parts entirely. This poses a challenge to the ICP procedure we use to align reconstructions to target meshes as we would be trying to align a partial reconstruction to a complete mesh, while relying on k -nearest neighbour search. To mitigate this, we use the object masks from the datasets to ignore any points during the ICP step, ground truth or reconstruction, that would be occluded in the given scene if rendered from the true camera view point. This mask is re-computed at every ICP iteration. As a result, we only align the visible parts of the object meshes. Furthermore, we noticed that objects with symmetry axes are sometimes misaligned, resulting in incorrect occlusion error calculations. We flip these objects to their correct rotation as this rotation

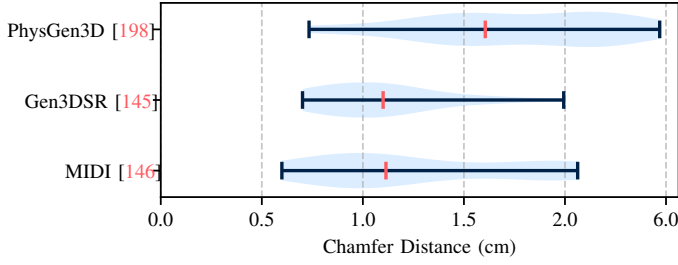


Fig. 5. Reconstruction error of scene reconstruction models on the YCB-Video [170] dataset as measured by the Chamfer distance (CD). CD is averaged across 10,000 sampled surface points from the entire scene reconstruction and target. Indicators for min, max, and median are shown. Reconstructed surfaces tend to be over 1cm distant from the closest target surface.

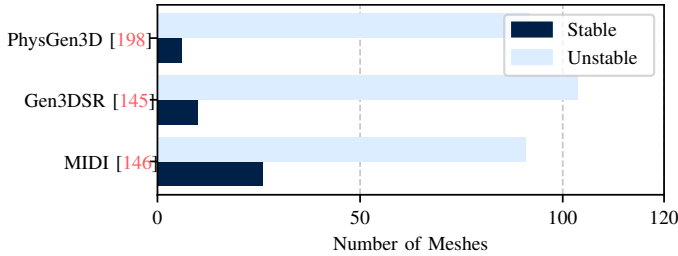


Fig. 7. Total number of objects with physically stable poses within 5° from the ground truth scene pose versus total number of objects without such stable poses. Evaluated on YCB-Video using scene reconstruction models. Only a small fraction of the objects show physically stable poses near those object poses that have been estimated by the scene reconstruction models.

misalignment is an artifact from the alignment process, not the reconstruction process. This ensures a fair comparison between methods. We evaluate how well the given reconstruction models estimate occluded structure by comparing the Chamfer distances of unoccluded object parts with the Chamfer distances of occluded object parts. Figure 9 shows that occlusion does lead to heavily increased reconstruction inaccuracy. The trend is consistent across all evaluated models with median Chamfer distances being between 40-95% higher at occluded regions. This is problematic for robotic manipulation as occluded object parts are often relevant for manipulation. Furthermore, when using such object reconstruction in simulation, the simulation would be based on a mesh that is not representative of the real-world object.

Scene reconstruction models fare much better in comparison. Figure 15 shows that across all models, the increase in median Chamfer distance is at most about 10%, with both MIDI [146] and PhysGen3D [198] being significantly below that threshold. MIDI considers objects jointly during reconstruction, and PhysGen3D and Gen3DSR both utilise image inpainting models to complete partial occlusions before mesh reconstruction. Both approaches appear well-suited for maintaining reconstruction accuracy at occluded object regions. For this evaluation, we individually aligned each reconstructed object to the target object mesh to avoid compounding error from erroneous pose estimations by the model, as shown in Figure 10.

e) *Computational and Memory Efficiency:* For evaluating computational cost, we measure the mean reconstruction time per object and the peak memory allocation during inference on the same data as used in our reconstruction accuracy evaluation.

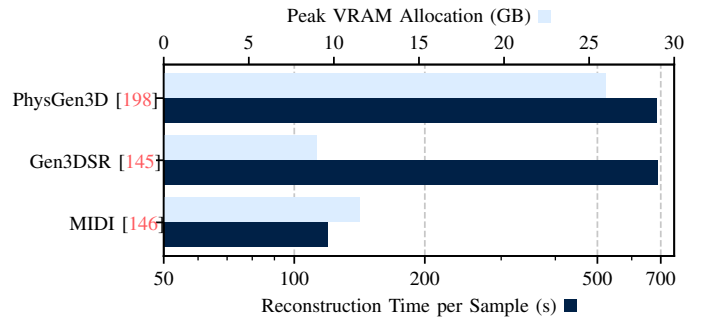


Fig. 6. Reconstruction time in seconds and memory utilisation for reconstructing entire scenes with multiple objects using different scene reconstruction models. While VRAM utilisation is roughly in line with what is reported for single-object models in Figure 11, the reconstruction time is an order of magnitude greater when operating on entire scenes. This effectively prohibits real-time execution when utilising such models.

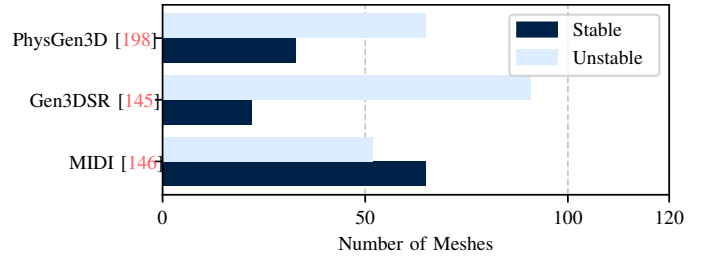


Fig. 8. Object stability as in Figure 7 but where each reconstructed object mesh is *separately* aligned with the target mesh, instead of relying on the relative object poses from the scene reconstruction model. Individual alignment results in a greater number of stable poses, indicating that the scene reconstruction models produce suboptimal object poses.

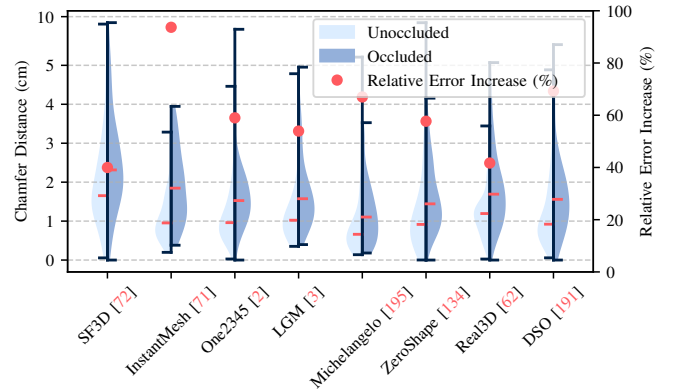


Fig. 9. Chamfer distances (CD) of unoccluded object parts versus occluded object parts. CD is averaged across unoccluded/unoccluded surface points from an initial set of 10,000 uniformly sampled surface points. Indicators for min, max, and median are shown. Occluded object regions result in significantly higher reconstruction error. This is a problem for robotics applications as occluded object parts are often relevant for manipulation. Furthermore, when using such object reconstruction in simulation, the simulation would be based on a mesh that is not representative of the real-world object.

All our experiments are run on a server node with four 2.1GHz CPU cores, 20GB of RAM, and a NVIDIA RTX A6000 GPU with 48GB of VRAM. We note that the VRAM capacity is roughly in line with what current NVIDIA Jetson devices offer for on-robot compute. However, our GPU is significantly faster overall and consequently, the reported compute times would likely be significantly higher if the models were deployed on a NVIDIA Jetson. Figure 11 depicts that most evaluated models take multiple, sometimes tens of seconds for reconstructing an individual object. SF3D [72] and ZeroShape [134] stand

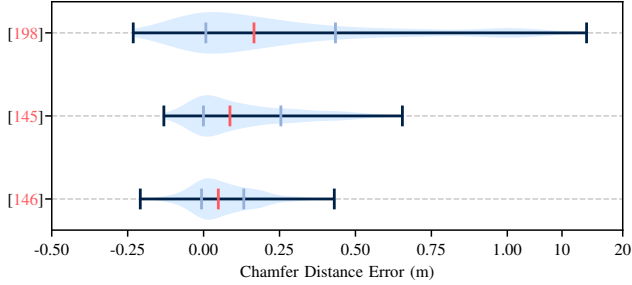


Fig. 10. Relative object position error of scene-level reconstruction models PhysGen3D [198], Gen3DSR [145], and MIDI [146]. Indicators for min, max, median, and 25th and 75th quantile are shown. We evaluate the difference between the Chamfer distances (CD) between all object pairs in the ground truth scene, and the CDs between the corresponding object pairs in the reconstructed scene with relative object poses estimated by the reconstruction models. Scene reconstruction models tend to overestimate relative object distances, resulting in inaccurate scene reconstructions and potentially impaired scene stability.

out by producing reconstruction within roughly 0.5 and 1 second, respectively. Still, reconstruction time scales linearly in the number of objects. We also observe large differences in memory allocation during inference. While SF3D [72], LGM [3], Michelangelo [195], and ZeroShape [134] all consume less than 10GB of VRAM, InstantMesh [116] and One2345 [2] require roughly triple and double the memory, respectively.

Comparing reconstruction error (Figures 1 and 13) and computational requirements (Figure 11), we do not observe a clear-cut trend that suggests computationally more expensive models, be it from having more parameters or generating multiple viewpoints, automatically produce more accurate reconstructions.

Scene reconstruction models require substantially more time to reconstruct their inputs than single-object reconstruction models (Figure 6). This appears sensible, as these models reconstruct multiple objects and also come with additional computational overhead to align reconstructed meshes. At the same time, VRAM utilisation is not too dissimilar to the single-object reconstruction models.

D. Limitations of the evaluation

While we have shown that the achieved reconstruction errors are too large for transferring grasps from simulation to the real world, the effect of reconstruction errors on the performance of robot manipulation tasks in general and on physical simulation is highly context-dependent. The task, target object, its surroundings, the type of robot gripper, and even the simulation engine all affect manipulation and simulation outcomes. As such, the question of precisely what error magnitude is permissible in a certain situation and whether any systematic relationship can be drawn up is an entire research question of itself and left for future work.

V. DISCUSSION AND AVENUES FOR FUTURE RESEARCH

In this paper, we evaluated the applicability of single-view 3D reconstruction models for creating digital twin environments in

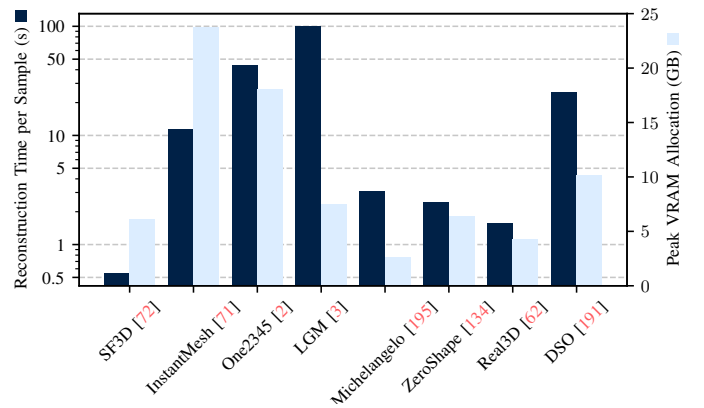


Fig. 11. Computational requirements during inference of all evaluated methods. The VRAM utilisation is in line what current on-device systems such as NVIDIA Jetson devices offer. However, the GPU used in this experiment is significantly faster than the Jetson devices. As such, the reconstruction time poses a major challenge for on-device systems as even on the more powerful evaluation system, reconstruction times are in the order of seconds. This is a major drawback for robotics applications that require real-time feedback.

robot manipulation tasks. Our systematic assessment against key desiderata revealed significant limitations in current approaches when applied to robotics scenarios. Despite impressive advancements in computer vision benchmarks, these models struggle with the practical constraints of robotics applications, including low-error reconstructions of typical robotic inputs, producing physically plausible and collision-free reconstructions, and managing occlusions in complex scenes.

The gap between computer vision capabilities and robotics requirements suggests several promising directions for future research. First, reconstruction models specifically trained on robotics-relevant data in addition to the current large-scale synthetic datasets could better address the input-domain-specific challenges we identified. In recent years, publications push for ever higher-resolution synthetic 3D datasets [39], [40]. However, robot practitioners often require models that are robust to noise due to sensor limitations, changing illumination conditions, lower resolution inputs, and partial views from non-canonical angles. Rather than focusing solely on increasing the resolution and visual fidelity of synthetic 3D assets, future datasets should incorporate more diverse capture conditions that reflect real-world robotics scenarios. This includes training with simulated sensor noise patterns, varied lighting conditions, realistic occlusions, and the lower-resolution imagery typical of on-robot cameras. Additionally, datasets should include more examples of objects viewed from challenging angles—such as top-down or bottom-up perspectives—which proved particularly problematic in our evaluation.

Second, the significant degradation in reconstruction quality between unoccluded and occluded object parts (40-95% higher Chamfer distances) further emphasises the need for training data that better represents partial visibility scenarios common in cluttered environments. Current scene-level reconstruction models tend to use image inpainting model in their pipelines, providing adequate results in our evaluation. Possible extensions in this direction could include physics-aware inpainting that considers how occluded parts must connect to visible portions while maintaining structural integrity. Training with synthetic

data that explicitly varies occlusion patterns would also help models learn more robust completion strategies.

We advise the robot practitioner against using single-object reconstruction models if objects tend to be physically close in the scene. Single-object reconstruction models by design do not consider spatial contexts and thus are not able to avoid collisions between reconstructed meshes. Scene reconstruction models, on the other hand, are able to leverage spatial context and thus should be preferred for reconstructing multiple objects in a scene. However, our evaluation shows that even scene reconstruction models struggle with producing physically plausible reconstructions. One reason for this certainly is that some scene-level reconstruction approaches [6], [145], [198] rely on single-object reconstruction models under the hood. MIDI [146] is an exception but does not show reduced object collisions either. A reason for this could be that while MIDI [146] is trained on a scene-level dataset, the training data only contains larger objects such as room-level furniture, and using models trained on these datasets on tabletop manipulation tasks is likely to result in poor performance. This is a major limitation as most robotic manipulation tasks are performed on smaller objects, such as those in the YCB-Video [170] dataset. This highlights a common issue of scene-level datasets that often times come in one of two flavours: either they are real-world datasets that do not contain true 3D annotations (only 2.5D) [167], [208], [209], or they are synthetic datasets resulting in a large domain gap between training and deployment environments [37], [40]. In our view, the ideal training dataset for robotics-oriented reconstruction would include both synthetic data for scale and diversity, and carefully curated real-world scene data with accurate ground-truth meshes to bridge the gap between training and deployment environments.

Object stability is another major limitation of current reconstruction models. While DSO [191] specifically trains for object stability, the authors set the threshold for object stability to 20° which is too large for most robotic manipulation tasks. Our evaluation shows that even the best-performing model, Michelangelo [195], only achieves a median object stability of about 65% on YCB-Video [170] and 40% on the Meta Aria Digital Twin [175] dataset. This is not sufficient for physical simulation, where object stability is crucial for scene integrity. We recommend that future models should be trained with a focus on object stability with tighter thresholds that are more in line with the requirements of robotic manipulation tasks.

More generally, we suggest that future models should incorporate depth information more explicitly in the reconstruction pipeline. Depth information is heavily commoditised in robotics due to the prevalence of RGB-D cameras [59] and consequently widely used in applications [212]–[214]. Depth information can resolve location/scale ambiguities and can give almost ground truth supervision signal about object shapes. But, as most low-cost RGB-D cameras rely on structured light projection, depth information is often incomplete or noisy at locations that are occluded from the depth infrared sensor but not the RGB sensor, at highly reflective surfaces, low-texture regions, or affected by external light sources. With depth completion being non-trivial [215], [216], reconstruction models should be able to cope with incomplete depth information, low depth

resolution, and depth misalignment. None of the evaluated models allow utilising 2.5D information from RGB-D cameras in their reconstruction pipeline by design. One could argue that some parts of their reconstruction pipelines could be adapted to incorporate real-world depth information. For example, One2345 [2] could be adapted such that the dense 3D volume on which the denoising process is run is initialised with depth information. Michelangelo [195] uses point clouds during pre-training to learn a latent space that merges shape, text, and image information. Again, one could consider initialising this latent space with point cloud information from observation before running the reverse diffusion process. Gen3DSR [145] appears most readily adaptable since it relies on a separate pre-trained model to predict a depth map which is then utilised to align objects with the observation. However, during exploratory experiments where we replaced the depth prediction model with the observed depth map from the RGB-D camera, we found that Gen3DSR is unable to handle missing depth values – a common issue with RGB-D cameras. Depth information offers a way of making the reconstruction process less ambiguous by providing information about the 3D structure of the scene. With depth information being commoditised in robotics, its utilisation in 3D reconstruction is a promising avenue towards more accurate reconstructions at almost no additional cost.

Our findings emphasise the need for closer collaboration between the computer vision and robotics communities to develop reconstruction techniques that specifically address the unique requirements of robot manipulation tasks.

ACKNOWLEDGMENTS

The authors thank Joe Watson, Jack Collins, Jun Yamada, and Alex Mitchell for fruitful discussions and valuable assistance in the preparation of this manuscript. This work is supported by the European Laboratory for Learning and Intelligent Systems and a UKRI/EPSCRC Programme Grant [EP/V000748/1]. We would also like to thank SCAN and ARC for use of their GPU acceleration facilities. Frederik Nolte is supported by the AWS Lighthouse Scholarship. Bernhard Schölkopf is a member of the Tübingen AI Center.

REFERENCES

- [1] R. Liu, R. Wu, B. Van Hoorick, P. Tokmakov, S. Zakharov, and C. Vondrick, “Zero-1-to-3: Zero-shot One Image to 3D Object,” 2023.
- [2] M. Liu, C. Xu, H. Jin, *et al.*, “One-2-3-45: Any Single Image to 3D Mesh in 45 Seconds without Per-Shape Optimization,” *Advances in Neural Information Processing Systems*, 2023.
- [3] J. Tang, Z. Chen, X. Chen, T. Wang, G. Zeng, and Z. Liu, “LGM: Large Multi-view Gaussian Model for High-Resolution 3D Content Creation,” in *Computer Vision – ECCV 2024*, 2025.
- [4] Y. Mu, T. Chen, S. Peng, *et al.*, *RoboTwin: Dual-Arm Robot Benchmark with Generative Digital Twins (early version)*, 2024.
- [5] A. Agarwal, G. Singh, B. Sen, T. Lozano-Pérez, and L. P. Kaelbling, *SceneComplete: Open-World 3D Scene Completion in Complex Real World Environments for Robot Manipulation*, 2024.
- [6] K. Yao, L. Zhang, X. Yan, *et al.*, *CAST: Component-Aligned 3D Scene Reconstruction from an RGB Image*, 2025.
- [7] P. Katara, Z. Xian, and K. Fragkiadaki, “Gen2Sim: Scaling up Robot Learning in Simulation with Generative Models,” in *2024 IEEE International Conference on Robotics and Automation (ICRA)*, 2024.
- [8] S. J. Qin and T. A. Badgwell, “A survey of industrial model predictive control technology,” *Control Engineering Practice*, 2003.
- [9] N. A. Hansen, H. Su, and X. Wang, “Temporal Difference Learning for Model Predictive Control,” in *Proceedings of the 39th International Conference on Machine Learning*, 2022.

- [10] R. Alterovitz, S. Koenig, and M. Likhachev, "Robot Planning in the Real World: Research Challenges and Opportunities," *AI Magazine*, 2016.
- [11] M. Suomalainen, Y. Karayiannidis, and V. Kyrki, "A survey of robot manipulation in contact," *Robotics and Autonomous Systems*, 2022.
- [12] F. Berkenkamp, M. Turchetta, A. Schoellig, and A. Krause, "Safe Model-based Reinforcement Learning with Stability Guarantees," in *Advances in Neural Information Processing Systems*, 2017.
- [13] M. O' Kelly, A. Sinha, H. Namkoong, R. Tedrake, and J. C. Duchi, "Scalable End-to-End Autonomous Vehicle Testing via Rare-event Simulation," in *Advances in Neural Information Processing Systems*, 2018.
- [14] L. Smith, I. Kostrikov, and S. Levine, "Demonstrating a walk in the park: Learning to walk in 20 minutes with model-free reinforcement learning," *Robotics: Science and Systems (RSS) Demo*, 2023.
- [15] N. Bohlinger, J. Kinzel, D. Palenicek, L. Antczak, and J. Peters, *Gait in Eight: Efficient On-Robot Learning for Omnidirectional Quadruped Locomotion*, 2025.
- [16] P. J. Ball, C. Lu, J. Parker-Holder, and S. Roberts, "Augmented World Models Facilitate Zero-Shot Dynamics Generalization From a Single Offline Environment," in *Proceedings of the 38th International Conference on Machine Learning*, 2021.
- [17] S. Prasanna, K. Farid, R. Rajan, and A. Biedenkapp, "Dreaming of Many Worlds: Learning Contextual World Models aids Zero-Shot Generalization," 2024.
- [18] L. Barcellona, A. Zadaianchuk, D. Allegro, S. Papa, S. Ghidoni, and E. Gavves, *Dream to Manipulate: Compositional World Models Empowering Robot Imitation Learning with Imagination*, 2024.
- [19] X. Han, M. Liu, Y. Chen, *et al.*, *Re³Sim: Generating High-Fidelity Simulation Data via 3D-Photorealistic Real-to-Sim for Robotic Manipulation*, 2025.
- [20] X. Li, J. Li, Z. Zhang, *et al.*, *RoboGSim: A Real2Sim2Real Robotic Gaussian Splatting Simulator*, 2024.
- [21] H. Lou, Y. Liu, Y. Pan, *et al.*, *Robo-GS: A Physics Consistent Spatial-Temporal Model for Robotic Arm with Hybrid Representation*, 2024.
- [22] Y. Wu, L. Pan, W. Wu, G. Wang, Y. Miao, and H. Wang, *RL-GSBridge: 3D Gaussian Splatting Based Real2Sim2Real Method for Robotic Manipulation Learning*, 2024.
- [23] M. N. Qureshi, S. Garg, F. Yandun, D. Held, G. Kantor, and A. Silwal, *SplatSim: Zero-Shot Sim2Real Transfer of RGB Manipulation Policies Using Gaussian Splatting*, 2024.
- [24] S. Zhu, L. Mou, D. Li, B. Ye, R. Huang, and H. Zhao, *VR-Robo: A Real-to-Sim-to-Real Framework for Visual Robot Navigation and Locomotion*, 2025.
- [25] Y. Jia, G. Wang, Y. Dong, *et al.*, *DISCOVERSE: Efficient Robot Simulation in Complex High-Fidelity Environments*, 2024.
- [26] M. Torne, A. Simeonov, Z. Li, *et al.*, *Reconciling Reality through Simulation: A Real-to-Sim-to-Real Approach for Robust Manipulation*, 2024.
- [27] S. Patel, X. Yin, W. Huang, *et al.*, "A Real-to-Sim-to-Real Approach to Robotic Manipulation with VLM-Generated Iterative Keypoint Rewards," 2024.
- [28] N. Pfaff, E. Fu, J. Binagia, P. Isola, and R. Tedrake, *Scalable Real2Sim: Physics-Aware Asset Generation Via Robotic Pick-and-Place Setups*, 2025.
- [29] Z. Meng, H. Qin, Z. Chen, *et al.*, "A Two-Stage Optimized Next-View Planning Framework for 3-D Unknown Environment Exploration, and Structural Reconstruction," *IEEE Robotics and Automation Letters*, 2017.
- [30] M. Breyer, L. Ott, R. Siegwart, and J. J. Chung, "Closed-Loop Next-Best-View Planning for Target-Driven Grasping," in *2022 IEEE/RSJ International Conference on Intelligent Robots and Systems (IROS)*, 2022.
- [31] J. Bohg, K. Hausman, B. Sankaran, *et al.*, "Interactive Perception: Leveraging Action in Perception and Perception in Action," *IEEE Transactions on Robotics*, 2017.
- [32] G. J. Pollayil, G. Grioli, M. Bonilla, and A. Bicchi, "Planning Robotic Manipulation with Tight Environment Constraints," in *2021 IEEE/RSJ International Conference on Intelligent Robots and Systems (IROS)*, 2021.
- [33] Y. Miao, R. Wang, and K. Bekris, "Safe, Occlusion-Aware Manipulation for Online Object Reconstruction in Confined Spaces," in *Robotics Research*, 2023.
- [34] E. Todorov, T. Erez, and Y. Tassa, "MuJoCo: A physics engine for model-based control," in *2012 IEEE/RSJ International Conference on Intelligent Robots and Systems*, 2012.
- [35] E. Coumans and Y. Bai, *Pybullet, a python module for physics simulation for games, robotics and machine learning*, 2016.
- [36] V. Makovychuk, L. Wawrzyniak, Y. Guo, *et al.*, "Isaac Gym: High Performance GPU Based Physics Simulation For Robot Learning," 2021.
- [37] A. X. Chang, T. Funkhouser, L. Guibas, *et al.*, *ShapeNet: An Information-Rich 3D Model Repository*, 2015.
- [38] J. Collins, S. Goel, K. Deng, *et al.*, "ABO: Dataset and Benchmarks for Real-World 3D Object Understanding," 2022.
- [39] T. Wu, J. Zhang, X. Fu, *et al.*, "OmniObject3D: Large-Vocabulary 3D Object Dataset for Realistic Perception, Reconstruction and Generation," 2023.
- [40] M. Deitke, R. Liu, M. Wallingford, *et al.*, "Objaverse-XL: A Universe of 10M+ 3D Objects," in *Advances in Neural Information Processing Systems*, 2023.
- [41] H. Wang, X. Du, J. Li, R. A. Yeh, and G. Shakhnarovich, "Score Jacobian Chaining: Lifting Pretrained 2D Diffusion Models for 3D Generation," 2023.
- [42] B. Poole, A. Jain, J. T. Barron, and B. Mildenhall, "DreamFusion: Text-to-3D using 2D Diffusion," 2022.
- [43] B. Maxim and S. Nedeveschi, "A survey on the current state of the art on deep learning 3D reconstruction," in *2021 IEEE 17th International Conference on Intelligent Computer Communication and Processing (ICCP)*, 2021.
- [44] M. G. Kantarci, B. Gökberk, and L. Akarun, "A Survey of 3D Object Reconstruction Methods," in *2022 30th Signal Processing and Communications Applications Conference (SIU)*, 2022.
- [45] Y. Bai, L. Wong, and T. Twan, *Survey on Fundamental Deep Learning 3D Reconstruction Techniques*, 2024.
- [46] C. Wang, M. A. Reza, V. Vats, *et al.*, "Deep learning-based 3D reconstruction from multiple images: A survey," *Neurocomputing*, 2024.
- [47] F. Remondino, A. Karami, Z. Yan, G. Mazzacca, S. Rigon, and R. Qin, "A Critical Analysis of NeRF-Based 3D Reconstruction," *Remote Sensing*, 2023.
- [48] B. Fei, J. Xu, R. Zhang, Q. Zhou, W. Yang, and Y. He, "3D Gaussian as a New Era: A Survey," *IEEE Transactions on Visualization and Computer Graphics*, 2024.
- [49] S. Zhu, G. Wang, X. Kong, D. Kong, and H. Wang, *3D Gaussian Splatting in Robotics: A Survey*, 2024.
- [50] Z. Chen, *A Review of Deep Learning-Powered Mesh Reconstruction Methods*, 2023.
- [51] N. Lei, Z. Li, Z. Xu, Y. Li, and X. Gu, "What's the Situation With Intelligent Mesh Generation: A Survey and Perspectives," *IEEE Transactions on Visualization and Computer Graphics*, 2024.
- [52] M. Z. Irshad, M. Comi, Y.-C. Lin, *et al.*, *Neural Fields in Robotics: A Survey*, 2024.
- [53] X. Zhang, Z. Li, S. Oymak, and J. Chen, "Text-to-3D Generative AI on Mobile Devices: Measurements and Optimizations," in *Proceedings of the 2023 Workshop on Emerging Multimedia Systems*, ser. EMS '23, 2023.
- [54] A. S. Morgan, B. Wen, J. Liang, A. Boularias, A. M. Dollar, and K. Bekris, "Vision-driven Compliant Manipulation for Reliable, High-Precision Assembly Tasks," in *17th Robotics: Science and Systems, RSS 2021*, 2021.
- [55] F. Zha, Y. Fu, P. Wang, *et al.*, "Semantic 3D Reconstruction for Robotic Manipulators with an Eye-In-Hand Vision System," *Applied Sciences*, 2020.
- [56] K. Ota, D. K. Jha, S. Jain, *et al.*, "Autonomous Robotic Assembly: From Part Singulation to Precise Assembly," in *2024 IEEE/RSJ International Conference on Intelligent Robots and Systems (IROS)*, 2024.
- [57] B. Niu, C. Wang, and C. Liu, "Tolerance-Guided Policy Learning for Adaptable and Transferrable Delicate Industrial Insertion," in *Proceedings of the 2020 Conference on Robot Learning*, 2021.
- [58] J. X.-Y. Lim and Q.-C. Pham, *Grasping, Part Identification, and Pose Refinement in One Shot with a Tactile Gripper*, 2023.
- [59] V. Tadic, A. Toth, Z. Vizvari, *et al.*, "Perspectives of RealSense and ZED Depth Sensors for Robotic Vision Applications," *Machines*, 2022.
- [60] D. Tochilkin, D. Pankratz, Z. Liu, *et al.*, *TripoSr: Fast 3D Object Reconstruction from a Single Image*, 2024.
- [61] Y. Liu, C. Lin, Z. Zeng, *et al.*, "SyncDreamer: Generating Multiview-consistent Images from a Single-view Image," 2023.
- [62] H. Jiang, Q. Huang, and G. Pavlakos, *Real3D: Scaling Up Large Reconstruction Models with Real-World Images*, 2024.
- [63] J. Ni, Y. Chen, B. Jing, *et al.*, "PhyRecon: Physically Plausible Neural Scene Reconstruction," 2024.

- [64] M. Guo, B. Wang, P. Ma, *et al.*, “Physically Compatible 3D Object Modeling from a Single Image,” in *Advances in Neural Information Processing Systems*, 2024.
- [65] Y. Chen, T. Xie, Z. Zong, *et al.*, “Atlas3D: Physically Constrained Self-Supporting Text-to-3D for Simulation and Fabrication,” 2024.
- [66] H. Yan, M. Zhang, Y. Li, C. Ma, and P. Ji, *PhyCAGE: Physically Plausible Compositional 3D Asset Generation from a Single Image*, 2024.
- [67] Y. Wang and H. Kasaei, “Learning Dual-Arm Push and Grasp Synergy in Dense Clutter,” *IEEE Robotics and Automation Letters*, 2025.
- [68] X. Kong, S. Liu, M. Taher, and A. J. Davison, “vMAP: Vectorised Object Mapping for Neural Field SLAM,” 2023.
- [69] Z. Li, X. Lyu, Y. Ding, M. Wang, Y. Liao, and Y. Liu, “RICO: Regularizing the Unobservable for Indoor Compositional Reconstruction,” 2023.
- [70] G. Qian, J. Mai, A. Hamdi, *et al.*, “Magic123: One Image to High-Quality 3D Object Generation Using Both 2D and 3D Diffusion Priors,” 2023.
- [71] J. Xu, W. Cheng, Y. Gao, X. Wang, S. Gao, and Y. Shan, *InstantMesh: Efficient 3D Mesh Generation from a Single Image with Sparse-view Large Reconstruction Models*, 2024.
- [72] M. Boss, Z. Huang, A. Vasishta, and V. Jampani, *SF3D: Stable Fast 3D Mesh Reconstruction with UV-unwrapping and Illumination Disentanglement*, 2024.
- [73] M. Liu, R. Shi, L. Chen, *et al.*, “One-2-3-45++: Fast Single Image to 3D Objects with Consistent Multi-View Generation and 3D Diffusion,” 2024.
- [74] A. Simpkins, “Real-time control in robotic systems,” in *Robotic Systems-Applications, Control and Programming*, 2012, p. 231.
- [75] E. Bylow, J. Sturm, C. Kerl, F. Kahl, and D. Cremers, “Real-time camera tracking and 3D reconstruction using signed distance functions,” in *Robotics: Science and systems (RSS) conference 2013*, 2013.
- [76] S. Izadi, D. Kim, O. Hilliges, *et al.*, “KinectFusion: Real-time 3D reconstruction and interaction using a moving depth camera,” in *Proceedings of the 24th annual ACM symposium on User interface software and technology*, ser. UIST ’11, 2011.
- [77] T. P. Swaminathan, C. Silver, and T. Akilan, *Benchmarking Deep Learning Models on NVIDIA Jetson Nano for Real-Time Systems: An Empirical Investigation*, 2024.
- [78] Y. S. Abdulsalam and M. Hedabou, “Security and Privacy in Cloud Computing: Technical Review,” *Future Internet*, 2022.
- [79] C.-H. Lin, C. Kong, and S. Lucey, “Learning Efficient Point Cloud Generation for Dense 3D Object Reconstruction,” *Proceedings of the AAAI Conference on Artificial Intelligence*, 2018.
- [80] P. Mandikal and V. B. Radhakrishnan, “Dense 3D Point Cloud Reconstruction Using a Deep Pyramid Network,” in *2019 IEEE Winter Conference on Applications of Computer Vision (WACV)*, 2019.
- [81] L. Melas-Kyriazi, C. Rupprecht, and A. Vedaldi, “PC2: Projection-Conditioned Point Cloud Diffusion for Single-Image 3D Reconstruction,” 2023.
- [82] A. Nichol, H. Jun, P. Dhariwal, P. Mishkin, and M. Chen, *Point-E: A System for Generating 3D Point Clouds from Complex Prompts*, 2022.
- [83] Z. Huang, Y. Wen, Z. Wang, J. Ren, and K. Jia, “Surface Reconstruction From Point Clouds: A Survey and a Benchmark,” *IEEE Transactions on Pattern Analysis and Machine Intelligence*, 2024.
- [84] M. Mittal, C. Yu, Q. Yu, *et al.*, “Orbit: A Unified Simulation Framework for Interactive Robot Learning Environments,” *IEEE Robotics and Automation Letters*, 2023.
- [85] J. K. Pontes, C. Kong, S. Sridharan, S. Lucey, A. Eriksson, and C. Fookes, “Image2Mesh: A Learning Framework for Single Image 3D Reconstruction,” in *Computer Vision – ACCV 2018*, 2019.
- [86] D. Jack, J. K. Pontes, S. Sridharan, *et al.*, “Learning Free-Form Deformations for 3D Object Reconstruction,” in *Computer Vision – ACCV 2018*, 2019.
- [87] N. Wang, Y. Zhang, Z. Li, Y. Fu, W. Liu, and Y.-G. Jiang, “Pixel2Mesh: Generating 3D Mesh Models from Single RGB Images,” 2018.
- [88] Y. Siddiqui, A. Alliegro, A. Artemov, *et al.*, “MeshGPT: Generating Triangle Meshes with Decoder-Only Transformers,” 2024.
- [89] A. Vaswani, N. Shazeer, N. Parmar, *et al.*, “Attention is All you Need,” in *Advances in Neural Information Processing Systems*, 2017.
- [90] T. Groueix, M. Fisher, V. G. Kim, B. C. Russell, and M. Aubry, “A Papier-Mâché Approach to Learning 3D Surface Generation,” 2018.
- [91] M. Mezghanni, M. Boulkenafed, A. Lieutier, and M. Ovsjanikov, “Physically-aware Generative Network for 3D Shape Modeling,” in *2021 IEEE/CVF Conference on Computer Vision and Pattern Recognition (CVPR)*, 2021.
- [92] R. Chen, Y. Chen, N. Jiao, and K. Jia, “Fantasia3D: Disentangling Geometry and Appearance for High-quality Text-to-3D Content Creation,” 2023.
- [93] B. Kerbl, G. Kopanas, T. Leimkuehler, and G. Drettakis, “3D Gaussian Splatting for Real-Time Radiance Field Rendering,” *ACM Trans. Graph.*, 2023.
- [94] L. Melas-Kyriazi, I. Laina, C. Rupprecht, *et al.*, “IM-3D: Iterative Multiview Diffusion and Reconstruction for High-Quality 3D Generation,” in *Proceedings of the 41st International Conference on Machine Learning*, 2024.
- [95] S. Szymanowicz, C. Rupprecht, and A. Vedaldi, “Splatter Image: Ultra-Fast Single-View 3D Reconstruction,” 2024.
- [96] Y. Xu, Z. Shi, W. Yifan, *et al.*, “GRM: Large Gaussian Reconstruction Model for Efficient 3D Reconstruction and Generation,” in *Computer Vision – ECCV 2024*, 2025.
- [97] D. Xu, Y. Yuan, M. Mardani, *et al.*, “AGG: Amortized Generative 3D Gaussians for Single Image to 3D,” *Transactions on Machine Learning Research*, 2024.
- [98] S. Szymanowicz, E. Insafutdinov, C. Zheng, *et al.*, *Flash3D: Feed-Forward Generalisable 3D Scene Reconstruction from a Single Image*, 2024.
- [99] L. Liu, X. Wang, J. Qiu, T. Lin, X. Zhou, and Z. Su, *Gaussian Object Carver: Object-Compositional Gaussian Splatting with surfaces completion*, 2024.
- [100] B. Mildenhall, P. P. Srinivasan, M. Tancik, J. T. Barron, R. Ramamoorthi, and R. Ng, “NeRF: Representing scenes as neural radiance fields for view synthesis,” *Communications of the ACM*, 2022.
- [101] J. J. Park, P. Florence, J. Straub, R. Newcombe, and S. Lovegrove, “DeepSDF: Learning Continuous Signed Distance Functions for Shape Representation,” 2019.
- [102] L. Mescheder, M. Oechsle, M. Niemeyer, S. Nowozin, and A. Geiger, “Occupancy Networks: Learning 3D Reconstruction in Function Space,” 2019.
- [103] C. Li, C. Zhang, A. Waghvase, *et al.*, “Generative AI meets 3D: A Survey on Text-to-3D in AIGC Era,” *CoRR*, 2023.
- [104] J. Aulinas, Y. Petillot, J. Salvi, Llado, and Xavier, “The SLAM problem: A survey,” in *Artificial Intelligence Research and Development*, 2008.
- [105] J. L. Schonberger and J.-M. Frahm, “Structure-From-Motion Revisited,” 2016.
- [106] B. Zheng, Y. Zhao, J. C. Yu, K. Ikeuchi, and S.-C. Zhu, “Beyond Point Clouds: Scene Understanding by Reasoning Geometry and Physics,” in *2013 IEEE Conference on Computer Vision and Pattern Recognition*, 2013.
- [107] Z. Yu, S. Peng, M. Niemeyer, T. Sattler, and A. Geiger, “MonoSDF: Exploring Monocular Geometric Cues for Neural Implicit Surface Reconstruction,” in *Advances in Neural Information Processing Systems*, 2022.
- [108] C. B. Choy, D. Xu, J. Gwak, K. Chen, and S. Savarese, “3D-R2N2: A Unified Approach for Single and Multi-view 3D Object Reconstruction,” in *Computer Vision – ECCV 2016*, 2016.
- [109] A. Kar, C. Häne, and J. Malik, “Learning a Multi-View Stereo Machine,” in *Advances in Neural Information Processing Systems*, 2017.
- [110] H. Xie, H. Yao, X. Sun, S. Zhou, and S. Zhang, “Pix2Vox: Context-Aware 3D Reconstruction From Single and Multi-View Images,” 2019.
- [111] D. P. Kingma and M. Welling, “Auto-Encoding Variational Bayes,” in *Proceedings of the International Conference on Learning Representations*, 2014.
- [112] D. Charatan, S. L. Li, A. Tagliasacchi, and V. Sitzmann, “pixelSplat: 3D Gaussian Splats from Image Pairs for Scalable Generalizable 3D Reconstruction,” 2024.
- [113] H. Chen, J. Gu, A. Chen, *et al.*, “Single-Stage Diffusion NeRF: A Unified Approach to 3D Generation and Reconstruction,” 2023.
- [114] H. Fan, H. Su, and L. J. Guibas, “A Point Set Generation Network for 3D Object Reconstruction From a Single Image,” 2017.
- [115] Y. Chen and X. Wang, “Transformers as Meta-learners for Implicit Neural Representations,” in *Computer Vision – ECCV 2022*, 2022.
- [116] J. Li, H. Tan, K. Zhang, *et al.*, “Instant3D: Fast Text-to-3D with Sparse-view Generation and Large Reconstruction Model,” 2023.
- [117] D. Pavllo, D. J. Tan, M.-J. Rakotosaona, and F. Tombari, “Shape, Pose, and Appearance From a Single Image via Bootstrapped Radiance Field Inversion,” 2023.
- [118] H.-H. Lee and A. X. Chang, *Understanding Pure CLIP Guidance for Voxel Grid NeRF Models*, 2022.
- [119] A. Jain, B. Mildenhall, J. T. Barron, P. Abbeel, and B. Poole, “Zero-Shot Text-Guided Object Generation With Dream Fields,” 2022.

- [120] Y. Shi, P. Wang, J. Ye, L. Mai, K. Li, and X. Yang, "MVDream: Multi-view Diffusion for 3D Generation," 2023.
- [121] Y. Chen, R. Xie, Q. Ye, *et al.*, *2L3: Lifting Imperfect Generated 2D Images into Accurate 3D*, 2024.
- [122] K. Wu, F. Liu, Z. Cai, *et al.*, "Unique3D: High-Quality and Efficient 3D Mesh Generation from a Single Image," 2024.
- [123] X.-F. Han, H. Laga, and M. Bennamoun, "Image-Based 3D Object Reconstruction: State-of-the-Art and Trends in the Deep Learning Era," *IEEE Transactions on Pattern Analysis and Machine Intelligence*, 2021.
- [124] O. Ronneberger, P. Fischer, and T. Brox, "U-Net: Convolutional Networks for Biomedical Image Segmentation," in *Medical Image Computing and Computer-Assisted Intervention – MICCAI 2015*, 2015.
- [125] M. Oquab, T. Darcet, T. Moutakanni, *et al.*, "DINOv2: Learning Robust Visual Features without Supervision," *Transactions on Machine Learning Research*, 2023.
- [126] K. He, X. Zhang, S. Ren, and J. Sun, "Deep Residual Learning for Image Recognition," 2016.
- [127] H. Jun and A. Nichol, *Shap-E: Generating Conditional 3D Implicit Functions*, 2023.
- [128] Y. Hong, K. Zhang, J. Gu, *et al.*, "LRM: Large Reconstruction Model for Single Image to 3D," 2023.
- [129] K. Rematas, R. Martin-Brualla, and V. Ferrari, "Sharf: Shape-conditioned Radiance Fields from a Single View," in *Proceedings of the 38th International Conference on Machine Learning*, 2021.
- [130] I. J. Goodfellow, J. Pouget-Abadie, M. Mirza, *et al.*, "Generative Adversarial Nets," in *Advances in Neural Information Processing Systems*, 2014.
- [131] T. Nguyen-Phuoc, C. Li, L. Theis, C. Richardt, and Y.-L. Yang, "HoloGAN: Unsupervised Learning of 3D Representations From Natural Images," 2019.
- [132] Y. Zhang, W. Chen, H. Ling, *et al.*, "Image GANs meet Differentiable Rendering for Inverse Graphics and Interpretable 3D Neural Rendering," 2020.
- [133] S. Rajeswar, F. Mannan, F. Golemo, D. Vazquez, D. Nowrouzezahrai, and A. Courville, "Pix2Scene: Learning Implicit 3D Representations from Images," 2018.
- [134] Z. Huang, S. Stojanov, A. Thai, V. Jampani, and J. M. Rehg, "ZeroShape: Regression-based Zero-shot Shape Reconstruction," 2024.
- [135] Y. Xu, H. Tan, F. Luan, *et al.*, "DMV3D: Denoising Multi-view Diffusion Using 3D Large Reconstruction Model," 2023.
- [136] P. Wang, H. Tan, S. Bi, *et al.*, "PF-LRM: Pose-Free Large Reconstruction Model for Joint Pose and Shape Prediction," 2023.
- [137] Z.-X. Zou, Z. Yu, Y.-C. Guo, *et al.*, "Triplane Meets Gaussian Splatting: Fast and Generalizable Single-View 3D Reconstruction with Transformers," 2024.
- [138] A. Radford, J. W. Kim, C. Hallacy, *et al.*, "Learning Transferable Visual Models From Natural Language Supervision," in *Proceedings of the 38th International Conference on Machine Learning*, 2021.
- [139] F. Hong, M. Zhang, L. Pan, Z. Cai, L. Yang, and Z. Liu, "AvatarCLIP: Zero-shot text-driven generation and animation of 3D avatars," *ACM Trans. Graph.*, 2022.
- [140] N. M. Khalid, T. Xie, E. Belilovsky, and T. Popa, "CLIP-Mesh: Generating textured meshes from text using pretrained image-text models," in *SIGGRAPH Asia 2022 Conference Papers*, 2022.
- [141] M. Yuksekgonul, F. Bianchi, P. Kalluri, D. Jurafsky, and J. Zou, "When and Why Vision-Language Models Behave like Bags-Of-Words, and What to Do About It?," 2022.
- [142] J. Wang, P. Wang, X. Long, *et al.*, "NeuRIS: Neural Reconstruction of Indoor Scenes Using Normal Priors," in *Computer Vision – ECCV 2022*, 2022.
- [143] M. Turkulainen, X. Ren, I. Melekhov, O. Seiskari, E. Rahtu, and J. Kannala, "DN-Splatter: Depth and Normal Priors for Gaussian Splatting and Meshing," in *2025 IEEE/CVF Winter Conference on Applications of Computer Vision (WACV)*, 2025.
- [144] S. Szymanowicz, J. Y. Zhang, P. Srinivasan, *et al.*, *Bolt3D: Generating 3D Scenes in Seconds*, 2025.
- [145] A. Dogaru, M. Özer, and B. Egger, *Generalizable 3D Scene Reconstruction via Divide and Conquer from a Single View*, 2024.
- [146] Z. Huang, Y.-C. Guo, X. An, *et al.*, *MIDI: Multi-Instance Diffusion for Single Image to 3D Scene Generation*, 2024.
- [147] H. Han, R. Yang, H. Liao, *et al.*, *REPARO: Compositional 3D Assets Generation with Differentiable 3D Layout Alignment*, 2024.
- [148] Q. Wu, X. Liu, Y. Chen, *et al.*, "Object-Compositional Neural Implicit Surfaces," in *Computer Vision – ECCV 2022*, 2022.
- [149] C. Zhang, Z. Cui, Y. Zhang, B. Zeng, M. Pollefeys, and S. Liu, "Holistic 3D Scene Understanding From a Single Image With Implicit Representation," 2021.
- [150] J. Chatterjee and M. Torres Vega, "3D-Scene-Former: 3D scene generation from a single RGB image using Transformers," *The Visual Computer*, 2024.
- [151] T. Wu, C. Zheng, Q. Wu, and T.-J. Cham, "ClusteringSDF: Self-Organized Neural Implicit Surfaces for 3D Decomposition," in *Computer Vision – ECCV 2024*, 2025.
- [152] G. Hassena, J. Moon, R. Fujii, *et al.*, *ObjectCarver: Semi-automatic segmentation, reconstruction and separation of 3D objects*, 2024.
- [153] M. Mezghanni, T. Bodrito, M. Boulkenafed, and M. Ovsjanikov, "Physical Simulation Layer for Accurate 3D Modeling," in *2022 IEEE/CVF Conference on Computer Vision and Pattern Recognition (CVPR)*, 2022.
- [154] Z. Chen, A. Walsman, M. Memmel, *et al.*, *URDFormer: A Pipeline for Constructing Articulated Simulation Environments from Real-World Images*, 2024.
- [155] L. Le, J. Xie, W. Liang, *et al.*, *Articulate-Anything: Automatic Modeling of Articulated Objects via a Vision-Language Foundation Model*, 2024.
- [156] R. Li, C. Zheng, C. Rupprecht, and A. Vedaldi, "DragAPart: Learning a Part-Level Motion Prior for Articulated Objects," in *Computer Vision – ECCV 2024*, 2025.
- [157] Y. Feng, Y. Shang, X. Li, T. Shao, C. Jiang, and Y. Yang, "PIE-NeRF: Physics-based Interactive Elastodynamics with NeRF," 2024.
- [158] C. Schuhmann, R. Beaumont, R. Vencu, *et al.*, "LAION-5B: An open large-scale dataset for training next generation image-text models," *Advances in Neural Information Processing Systems*, 2022.
- [159] A. Kirillov, E. Mintun, N. Ravi, *et al.*, "Segment Anything," 2023.
- [160] J. M. Patel, "Introduction to Common Crawl Datasets," in *Getting Structured Data from the Internet: Running Web Crawlers/Scrapers on a Big Data Production Scale*, 2020.
- [161] L. Downs, A. Francis, N. Koenig, *et al.*, "Google Scanned Objects: A High-Quality Dataset of 3D Scanned Household Items," in *2022 International Conference on Robotics and Automation (ICRA)*, 2022.
- [162] T. Jaunet, G. Bono, R. Vuillemot, and C. Wolf, *SIM2REALVIZ: Visualizing the Sim2Real Gap in Robot Ego-Pose Estimation*, 2021.
- [163] M. Khanna, Y. Mao, H. Jiang, *et al.*, "Habitat Synthetic Scenes Dataset (HSSD-200): An Analysis of 3D Scene Scale and Realism Tradeoffs for ObjectGoal Navigation," 2024.
- [164] E. Kolve, R. Mottaghi, W. Han, *et al.*, *AI2-THOR: An Interactive 3D Environment for Visual AI*, 2022.
- [165] M. Deitke, E. VanderBilt, A. Herrasti, *et al.*, "ProcTHOR: Large-Scale Embodied AI Using Procedural Generation," *Advances in Neural Information Processing Systems*, 2022.
- [166] M. Deitke, W. Han, A. Herrasti, *et al.*, "RoboTHOR: An Open Simulation-to-Real Embodied AI Platform," 2020.
- [167] A. Chang, A. Dai, T. Funkhouser, *et al.*, "Matterport3D: Learning from RGB-D Data in Indoor Environments," 2017.
- [168] G. Baruch, Z. Chen, A. Dehghan, *et al.*, "ARKitScenes: A Diverse Real-World Dataset For 3D Indoor Scene Understanding Using Mobile RGB-D Data," 2021.
- [169] J. Sturm, N. Engelhard, F. Endres, W. Burgard, and D. Cremers, "A benchmark for the evaluation of RGB-D SLAM systems," in *2012 IEEE/RSJ International Conference on Intelligent Robots and Systems*, 2012.
- [170] Y. Xiang, T. Schmidt, V. Narayanan, and D. Fox, "PoseCNN: A Convolutional Neural Network for 6D Object Pose Estimation in Cluttered Scenes," 2018.
- [171] B. Calli, A. Singh, A. Walsman, S. Srinivasa, P. Abbeel, and A. M. Dollar, "The YCB object and Model set: Towards common benchmarks for manipulation research," in *2015 International Conference on Advanced Robotics (ICAR)*, 2015.
- [172] X. Deng, Y. Xiang, A. Mousavian, C. Eppner, T. Bretl, and D. Fox, "Self-supervised 6D Object Pose Estimation for Robot Manipulation," in *2020 IEEE International Conference on Robotics and Automation (ICRA)*, 2020.
- [173] Q. Lu, N. Baron, A. B. Clark, and N. Rojas, "Systematic object-invariant in-hand manipulation via reconfigurable underactuation: Introducing the RUTH gripper," *The International Journal of Robotics Research*, 2021.
- [174] T. Lerher, P. Bencak, D. Hercog, B. Jerman, and L. Bizjak, "Robotic bin-picking: Benchmarking robotics grippers with modified YCB object and model set," *Progress in Material Handling Research*, 2023.
- [175] X. Pan, N. Charron, Y. Yang, *et al.*, "Aria Digital Twin: A New Benchmark Dataset for Egocentric 3D Machine Perception," 2023.

- [176] X. Yue, Y. Zhang, J. Chen, J. Chen, X. Zhou, and M. He, "LiDAR-based SLAM for robotic mapping: State of the art and new frontiers," *Industrial Robot: the international journal of robotics research and application*, 2024.
- [177] B. Al-Tawil, T. Hempel, A. Abdelrahman, and A. Al-Hamadi, "A review of visual SLAM for robotics: Evolution, properties, and future applications," *Frontiers in Robotics and AI*, 2024.
- [178] E. Šlapak, E. Pardo, M. Dopirak, T. Maksymyuk, and J. Gazda, "Neural radiance fields in the industrial and robotics domain: Applications, research opportunities and use cases," *Robotics and Computer-Integrated Manufacturing*, 2024.
- [179] H. Temeltas and D. Kayak, "SLAM for robot navigation," *IEEE Aerospace and Electronic Systems Magazine*, 2008.
- [180] C. Cadena, L. Carlone, H. Carrillo, *et al.*, "Past, Present, and Future of Simultaneous Localization and Mapping: Toward the Robust-Perception Age," *IEEE Transactions on Robotics*, 2016.
- [181] D. Damjanović, P. Biočić, S. Praljačić, D. Činčurak, and J. Balen, "A comprehensive survey on SLAM and machine learning approaches for indoor autonomous navigation of mobile robots," *Machine Vision and Applications*, 2025.
- [182] J. Abou-Chakra, K. Rana, F. Dayoub, and N. Sünderhauf, *Physically Embodied Gaussian Splatting: A Realtime Correctable World Model for Robotics*, 2024.
- [183] OpenAI *et al.*, *GPT-4 Technical Report*, 2024.
- [184] G. Lu, S. Zhang, Z. Wang, C. Liu, J. Lu, and Y. Tang, "ManiGaussian: Dynamic Gaussian Splatting for Multi-task Robotic Manipulation," in *Computer Vision – ECCV 2024*, 2025.
- [185] T. Wu, C. Zheng, F. Guan, A. Vedaldi, and T.-J. Cham, *Amodal 3D Reconstruction from Occluded 2D Images*, 2025.
- [186] T. Chu, P. Zhang, Q. Liu, and J. Wang, "BUOL: A Bottom-Up Framework With Occupancy-Aware Lifting for Panoptic 3D Scene Reconstruction From a Single Image," 2023.
- [187] L. Zhang, Z. Wang, Q. Zhang, *et al.*, "CLAY: A Controllable Large-scale Generative Model for Creating High-quality 3D Assets," *ACM Trans. Graph.*, 2024.
- [188] H. Wu, M. G. Karumuri, C. Zou, *et al.*, *Direct and Explicit 3D Generation from a Single Image*, 2024.
- [189] J. Sun, B. Zhang, R. Shao, *et al.*, "DreamCraft3D: Hierarchical 3D Generation with Bootstrapped Diffusion Prior," 2023.
- [190] J. Tang, J. Ren, H. Zhou, Z. Liu, and G. Zeng, "DreamGaussian: Generative Gaussian Splatting for Efficient 3D Content Creation," 2023.
- [191] R. Li, C. Zheng, C. Rupprecht, and A. Vedaldi, *DSO: Aligning 3D Generators with Simulation Feedback for Physical Soundness*, 2025.
- [192] Q. Shen, Z. Wu, X. Yi, *et al.*, *Gamba: Marry Gaussian Splatting with Mamba for single view 3D reconstruction*, 2024.
- [193] L. Lu, H. Gao, T. Dai, *et al.*, "Large Point-to-Gaussian Model for Image-to-3D Generation," in *Proceedings of the 32nd ACM International Conference on Multimedia*, ser. MM '24, 2024.
- [194] X. Wei, K. Zhang, S. Bi, *et al.*, *MeshLRM: Large Reconstruction Model for High-Quality Meshes*, 2025.
- [195] Z. Zhao, W. Liu, X. Chen, *et al.*, "Michelangelo: Conditional 3D Shape Generation based on Shape-Image-Text Aligned Latent Representation," in *Advances in Neural Information Processing Systems*, 2023.
- [196] C.-Y. Wu, J. Johnson, J. Malik, C. Feichtenhofer, and G. Gkioxari, "Multiview Compressive Coding for 3D Reconstruction," 2023.
- [197] M. Wen and K. Cho, "Object-Aware 3D Scene Reconstruction from Single 2D Images of Indoor Scenes," *Mathematics*, 2023.
- [198] B. Chen, H. Jiang, S. Liu, *et al.*, *PhysGen3D: Crafting a Miniature Interactive World from a Single Image*, 2025.
- [199] Y. Chen, J. Ni, N. Jiang, Y. Zhang, Y. Zhu, and S. Huang, "Single-view 3D Scene Reconstruction with High-fidelity Shape and Texture," in *2024 International Conference on 3D Vision (3DV)*, 2024.
- [200] V. Voleti, C.-H. Yao, M. Boss, *et al.*, "SV3D: Novel Multi-view Synthesis and 3D Generation from a Single Image Using Latent Video Diffusion," in *Computer Vision – ECCV 2024*, 2025.
- [201] Z. Qi, M. Yu, R. Dong, and K. Ma, "VPP: Efficient Conditional 3D Generation via Voxel-Point Progressive Representation," in *Advances in Neural Information Processing Systems*, 2023.
- [202] X. Long, Y.-C. Guo, C. Lin, *et al.*, "Wonder3D: Single Image to 3D using Cross-Domain Diffusion," 2024.
- [203] T. Chabal, S. Chen, J. Ponce, and C. Schmid, "Online 3D Scene Reconstruction Using Neural Object Priors," in *3DV 2025 - 12th International Conference on 3D Vision 2025*, 2025.
- [204] Y. Jiang, C. Yu, T. Xie, *et al.*, "VR-GS: A Physical Dynamics-Aware Interactive Gaussian Splatting System in Virtual Reality," in *ACM SIGGRAPH 2024 Conference Papers*, ser. SIGGRAPH '24, 2024.
- [205] B. Huang, Z. Yu, A. Chen, A. Geiger, and S. Gao, "2D Gaussian Splatting for Geometrically Accurate Radiance Fields," in *ACM SIGGRAPH 2024 Conference Papers*, ser. SIGGRAPH '24, 2024.
- [206] W. Kim, J. Park, and K. Cho, "Complete Object-Compositional Neural Implicit Surfaces With 3D Pseudo Supervision," *IEEE Access*, 2025.
- [207] R. Wu, B. Mildenhall, P. Henzler, *et al.*, "ReconFusion: 3D Reconstruction with Diffusion Priors," 2024.
- [208] N. Silberman, D. Hoiem, P. Kohli, and R. Fergus, "Indoor Segmentation and Support Inference from RGBD Images," in *Computer Vision – ECCV 2012*, 2012.
- [209] A. Dai, A. X. Chang, M. Savva, M. Halber, T. Funkhouser, and M. Niessner, "ScanNet: Richly-Annotated 3D Reconstructions of Indoor Scenes," 2017.
- [210] M. Gilles, Y. Chen, T. Robin Winter, E. Zhixuan Zeng, and A. Wong, "MetaGraspNet: A Large-Scale Benchmark Dataset for Scene-Aware Ambidextrous Bin Picking via Physics-based Metaverse Synthesis," in *2022 IEEE 18th International Conference on Automation Science and Engineering (CASE)*, 2022.
- [211] J. Pan, S. Chitta, and D. Manocha, "FCL: A general purpose library for collision and proximity queries," in *2012 IEEE International Conference on Robotics and Automation*, 2012.
- [212] S. Wei, H. Geng, J. Chen, *et al.*, "D³RoMa: Disparity Diffusion-based Depth Sensing for Material-Agnostic Robotic Manipulation," 2024.
- [213] J. Li, W. Wang, Y. Peng, C. Shen, Y. Zhu, and Z. Xu, "Visual Robotic Manipulation with Depth-Aware Pretraining," in *2024 IEEE International Conference on Robotics and Biomimetics (ROBIO)*, 2024.
- [214] D. Kent, C. Saldanha, and S. Chernova, "Leveraging depth data in remote robot teleoperation interfaces for general object manipulation," *The International Journal of Robotics Research*, 2020.
- [215] Y. Zhang and T. Funkhouser, "Deep Depth Completion of a Single RGB-D Image," 2018.
- [216] M. A. U. Khan, D. Nazir, A. Pagani, *et al.*, "A comprehensive survey of depth completion approaches," *Sensors*, 2022.
- [217] E. R. Chan, C. Z. Lin, M. A. Chan, *et al.*, "Efficient Geometry-Aware 3D Generative Adversarial Networks," 2022.
- [218] T. Shen, J. Gao, K. Yin, M.-Y. Liu, and S. Fidler, "Deep Marching Tetrahedra: A Hybrid Representation for High-Resolution 3D Shape Synthesis," in *Advances in Neural Information Processing Systems*, 2021.
- [219] J. Xiang, Z. Lv, S. Xu, *et al.*, *Structured 3D Latents for Scalable and Versatile 3D Generation*, 2025.
- [220] M. FISCHLER AND, "Random sample consensus: A paradigm for model fitting with applications to image analysis and automated cartography," *Commun. ACM*, 1981.

VI. BIOGRAPHY SECTION

Frederik Nolte is an ELLIS PhD student currently pursuing a DPhil in Engineering Science in the Applied AI Lab at the Oxford Robotics Institute. Previously, he earned an M.Sc. in Artificial Intelligence from the University of Amsterdam, where he was an ELLIS Honours Student.

Bernhard Schölkopf (Senior Member, IEEE) received degrees in mathematics (University of London, U.K., 1992), physics (University of Tübingen, Germany, 1994), and a Ph.D. in computer science (Technische Universität Berlin, Germany, 1997). He has researched at AT&T Bell Labs, Microsoft Research Cambridge, and Amazon. He is Director at the MPI for Intelligent Systems and at the ELLIS Institute Tübingen, Germany, and professor at ETH Zürich. His scientific interests include machine learning, causal inference and their applications across the sciences. Schölkopf received the Royal Society Milner Award, the Leibniz Prize, the Körber Prize, and the ACM AAAI Allen Newell Award.

Ingmar Posner (Member, IEEE) leads the Applied Artificial Intelligence Lab (A2I) at Oxford University and served as a Founding Director of the Oxford Robotics Institute (ORI). His research aims to enable machines to robustly act and interact in the real world - for, with, and alongside humans. It includes seminal work on large-scale learning from demonstration, unsupervised learning of scene dynamics and 3D object detection. Currently, Ingmar's research focusses on representation learning for real-to-sim applications and world models in robotics and beyond. He is the recipient of a number of best paper awards at recognised international venues in robotics and AI such as ICAPS, IROS and ISER. An ELLIS Fellow, in 2014 he co-founded Oxa, a multi-award winning provider of mobile autonomy software solutions. He currently serves as an Amazon Scholar.

APPENDIX

a) Object-Level Reconstruction Models:

SF3D [72]: Extends TripoSR [60] by adding material and lighting estimation. Uses a transformer to predict a Triplane [217], which is meshed via differentiable Marching Tetrahedron [218].

InstantMesh [116]: Uses a multi-view diffusion model to generate views, which are encoded into Triplane [217] features. These features are then converted into meshes.

One2345 [2]: Produces dense multi-view images via diffusion, then aggregates them into a discretized volume. This is converted into a signed distance function and finally meshed.

LGM [3]: Generates multi-view images with diffusion and processes them via U-Net [124] into 3D Gaussians. These are rendered to train a NeRF [100], which is used for mesh extraction.

Michelangelo [195]: Combines image, shape, and text in a latent autoencoder, followed by diffusion-based shape sampling. A conditioned occupancy network then extracts meshes.

ZeroShape [134]: Estimates depth and camera intrinsics to project the image into 3D space. A conditional occupancy network processes this for mesh generation.

Real3D [62]: Builds on TripoSR [60] and incorporates real-world data using an unsupervised loss. This co-training reduces domain shift and improves performance on real data.

DSO [191]: Fine-tunes TRELIS [219] with a physics-informed reward system for stable 3D shapes. TRELIS encodes images into structured latents, decoded into SDFs for mesh extraction.

b) Scene-Level Reconstruction Models:

MIDI [146]: Segments all objects in the scene using an image segmentation model. Then denoises latent embeddings jointly across objects using cross-instance self-attention, improving spatial reasoning. This enhances the model’s understanding of object relationships in the scene.

Gen3DSR [145]: Segments and inpaints occluded objects before applying single-object 3D reconstruction. Aligns meshes to the scene using RANSAC [220] between object meshes and estimated depth. Background reconstruction is omitted for fair comparison in experiments.

PhysGen3D [198]: Segments, inpaints, and reconstructs objects with InstantMesh [71]. Aligns them using keypoint descriptors and a differentiable renderer for refined pose. Adds language-model-inferred physical properties but does not handle collisions or stability during reconstruction.

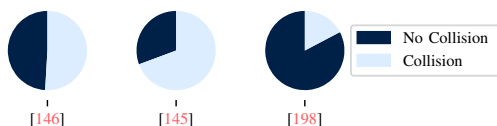


Fig. 12. Ratio of number of objects in collision to number of objects not in collision, averaged over a dataset of 28 YCB-Video [170] scenes. Even though scene reconstruction models have access to information about the entire scene, mesh collisions in 3D reconstruction are common. PhysGen3D [198] is more successful at avoiding object collisions. However, this could be an artifact from the model tending to markedly overestimate relative object distances (see Figure 10), thus erroneously pushing objects apart and avoiding collisions.

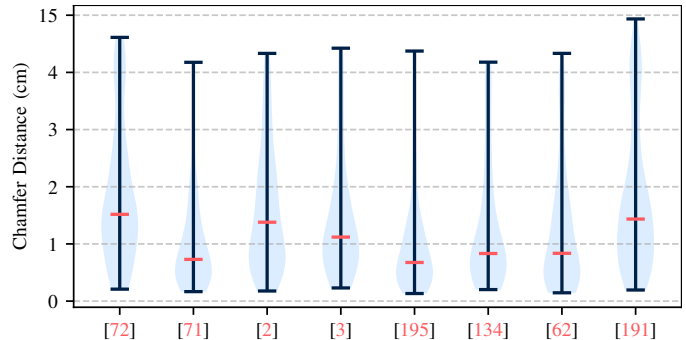


Fig. 13. Reconstruction error on the Meta Aria Digital Twin [175] dataset as measured by the Chamfer distance (CD). CD is averaged across 10,000 sampled surface points from both target and reconstruction. Indicators for min, max, and median are shown. Reconstruction errors on this dataset are noticeably higher than those shown in Figure 1. Reconstructed surfaces tend to be 1cm distant from the closest target mesh surface.

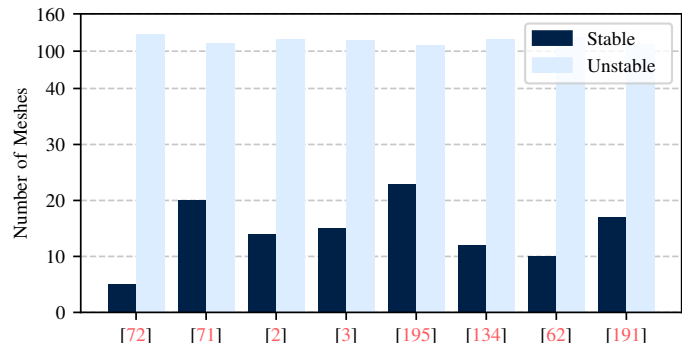


Fig. 14. Total number of objects with physically stable poses within 5° from the ground truth scene pose versus total number of objects without such stable poses. Evaluated on the Aria Digital Twin [175] dataset. Similar to the results on the YCB-Video [170] dataset, most reconstructed object meshes across all methods lack the physical stability required for accurate simulation. When incorporated into physics engines, these unstable geometries cause entire scene reconstructions to collapse rather than maintain their intended configurations.

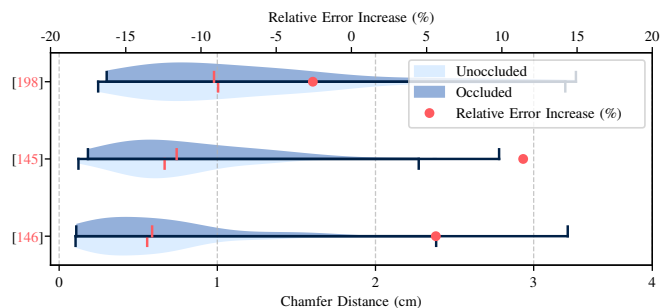


Fig. 15. Chamfer distances (CD) of unoccluded object parts versus occluded object parts for scene-level reconstruction models. CD is averaged across occluded/unoccluded surface points from an initial set of 10,000 uniformly sampled surface points. To avoid error propagation from incorrect relative pose estimation on the reconstruction models’ part, we individually align each reconstructed object with its target mesh at the corresponding scene pose using the masked ICP procedure described in Section IV-B. Indicators for min, max, and median are shown. Gen3DSR [145] and PhysGen3D [198] rely on image in-painting to resolve occlusions, whereas MIDI [146] uses a custom shared denoising process to condition objects on one another. Both approaches result in noticeable improvements over single-object reconstruction models without any such procedures (see Figure 9). We conclude that scene-level information can be highly beneficial for resolving object occlusions.

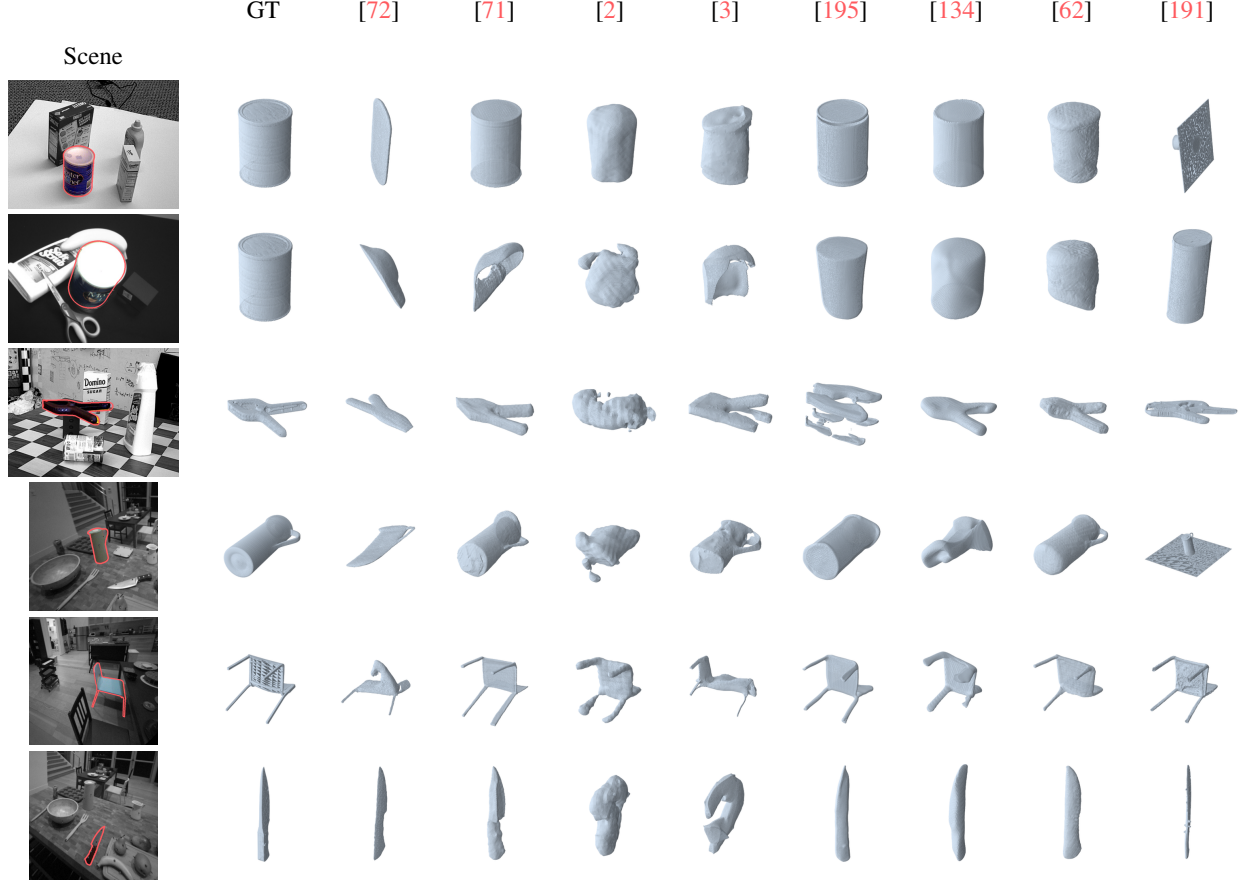


Fig. 16. Sample reconstructions on the YCB-Video [170] dataset (rows 1, 2, 3) and the Meta Aria Digital Twin [175] dataset (rows 4, 5, 6) using different 3D reconstruction methods. Reconstruction target objects are contoured and coloured. The scene renderings are solely for context as the reconstruction models are only given the segmented target object on transparent background. We observe that models tend to perform better on simple object shapes from highly informative viewpoints. Non-standard objects and more extreme viewpoints result in markedly lower reconstruction accuracy (compare rows 1, 2). Reconstruction quality on the Aria dataset is arguably lower than on YCB-Video. Objects in the Aria dataset tend to occupy less space on the image plane, resulting in less visual information in the model inputs.

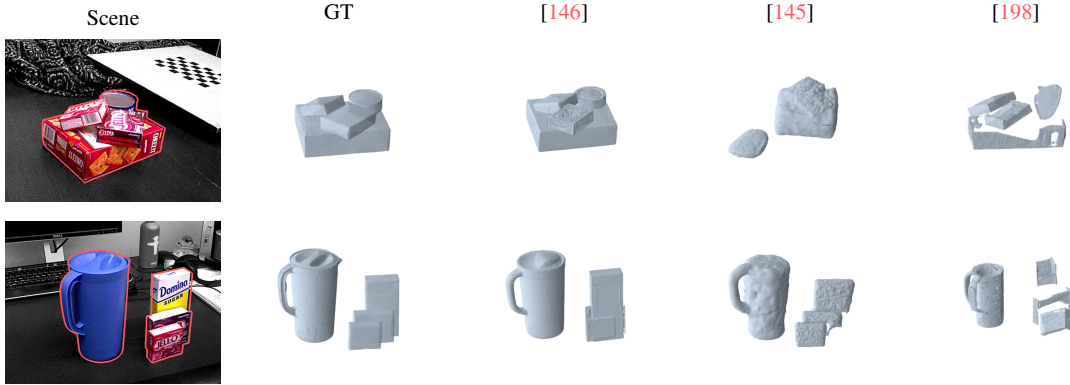


Fig. 17. YCB-Video [170] scene reconstructions using different 3D reconstruction methods that process multi-object scenes. The objects that are reconstructed are shown contoured and in colour. The scene renderings are solely for context as the reconstruction models are only given the segmented target objects on transparent background. Scene reconstruction models struggle not only with object reconstruction quality but also accurate object pose estimation, resulting in mesh collisions and levitating objects.